

MODELLING AND SIMULATION OF SIDE
MILLING PROCESS USING FINITE ELEMENT
ANALYSIS

WONG CHOON FUAN

BACHELOR OF ENGINEERING
UNIVERSITY MALAYSIA PAHANG

**MODELLING AND SIMULATION OF SIDE
MILLING USING FINITE ELEMENT ANALYSIS**

WONG CHOON FUAN

Report submitted in partial fulfillment of the requirements
for the award of the degree of
Bachelor of Engineering in Manufacturing Engineering

Faculty of Manufacturing Engineering

UNIVERSITI MALAYSIA PAHANG

June 2016

SUPERVISOR'S DECLARATION

I hereby declare that I have checked this thesis and in my opinion, this thesis is adequate in terms of scope and quality for the award of the degree of Bachelor of Engineering in Manufacturing.

Signature :

Name of supervisor : Dr. Mebrahitom Asmelash Gebremariam

Position :

Date :

STUDENT'S DECLARATION

I hereby declare that the work in this thesis is my own except for quotation and summaries which have been duly acknowledged. The thesis has not been accepted for any degree and is not concurrently submitted for award of other degree.

Signature :

Name : Wong Choon Fuan

ID Number : FA12058

Date :

ACKNOWLEDGEMENTS

First of all, I would like to express my sincere gratitude to my supervisor Dr Asmelash Mebrahitom for his treasure ideas, valuable guidance, continuous encouragement and constant support in making this research possible. He has been the teacher and partner for the path of this research. He has always guided me with his outstanding professional knowledge, his strong persuasion for science. I really appreciate him for the support consistently from the day I had been assigned with this title. I am truly grateful for his tolerance of some of my mistakes, and also the commitment of him to try to help in my future career. I would like to say thank you to my supervisor Dr Asmelash Mebrahitom with his advices and guidance.

Next, I would like to give my sincere appreciation to all my lab mates and the staff members of Manufacturing Engineering Department and Mechanical Engineering Department, UMP, who really helped a lot in many aspects and the progression of my research. I would like to thanks to their excellent co-operation and supports during my study of this research.

I acknowledge my sincere liability and gratitude to my parents for their love, sacrifice and dream throughout my life. I acknowledge my sincere appreciation to my parents, who consistently encouraged me throughout the research of this title. I am also grateful to my brothers for their understanding, patience that were undeniably to make this work possible. I couldn't find any words to describe how I appreciate who support and encourage in my ability to achieve my goals. I would like to acknowledge their commitments and suggestions, which was truly crucial for the completion of this study.

ABSTRACT

This ~~thesis project~~ deals with modelling and simulation of side milling using Finite Element Analysis. The ~~objectives of this thesis is~~ ~~objective of this thesis is~~ to validate the cutting force result between simulation and experiment. ~~The thesis~~ It describes how the finite element ~~analysis predict~~ ~~analysis predicts~~ the cutting force before the machining process is proceed~~ed~~. The data ~~we obtained~~ in this project ~~is~~ ~~were~~ cutting force and stress during the side milling process. Machining parameters such as cutting speed, feed rate, spindle speed were ~~also studied~~ ~~in this thesis which commonly will be decide before experiment and simulation started~~. The cutting force and stress prediction was done by using finite element analysis ~~which is~~ ~~software called~~ ABAQUS. ~~The strategy of validation of finite element model was developed. The finite element analysis was then performed based on the side milling orientation.~~ The finite element analysis was analyzed based on the interaction between aluminium 6061 ~~work piece~~ and high speed steel ~~tool cutter~~. The ~~experiment was then performed~~ ~~cutting forces were measured~~ by using dynamometer ~~to obtain the cutting force during~~ ~~during~~ the side milling process. The machining parameters ~~was~~ ~~were~~ calculated before the experiment ~~carry on~~ ~~started~~. Finally, the cutting force in the three ~~direction~~ ~~directions~~ which is X, Y and Z direction versus time was measured and recorded in the data acquisition software which is Dyno-ware. From the results of dynamometer, noise has been eliminated to get the certain time period of cutting force. ~~Finally, the~~ ~~The~~ results between simulation and experiment indicates ~~that that the optimization of machining processes can be done by~~ ~~the predicting~~ ~~predicted and~~ the ~~measured~~ cutting force of milling process ~~and also observe the chip formation~~ ~~are in a good agreement~~.

Formatted: Font: 12 pt

Formatted: Font: 12 pt

Formatted: Font: 12 pt

Formatted: Font: 12 pt

Formatted: Font: 12 pt

Formatted: Font: 12 pt

Formatted: Font: 12 pt

Formatted: Font: 12 pt

ABSTRAK

Tesis ini berkaitan dengan pemodelan dan simulasi pengilangan sampingan menggunakan terhingga Analisis Element. Objektif projek ini adalah untuk mengesahkan hasil daya pemotongan antara simulasi dan eksperimen. tesis ini menerangkan bagaimana analisis unsur terhingga meramalkan daya pemotongan sebelum proses pemesinan adalah meneruskan. Data yang kami mendapatkan dalam projek ini adalah memotong kekerasan dan tekanan semasa proses sisi pengilangan. parameter pemesinan seperti kelajuan pemotongan, kadar suapan, kelajuan gelendong telah dikaji dalam tesis ini yang biasanya akan membuat keputusan sebelum eksperimen dan simulasi memulakan. Daya pemotongan dan tekanan ramalan telah dilakukan dengan menggunakan analisis unsur terhingga yang Abaqus. Strategi pengesahan model unsur terhingga telah dibangunkan. analisis unsur terhingga kemudian dilaksanakan berdasarkan orientasi sisi pengilangan. analisis unsur terhingga telah dianalisis berasaskan interaksi antara aluminium 6061 dan keluli kelajuan tinggi. Eksperimen kemudian dilakukan dengan menggunakan dinamometer untuk mendapatkan daya pemotongan semasa proses sisi pengilangan. Parameter pemesinan dikira sebelum percubaan dijalankan. Akhir sekali, daya pemotongan ke arah yang tiga yang X, Y dan Z arah melawan masa diukur dan direkodkan dalam perisian perolehan data yang Dyno-ware. Dari hasil dinamometer, bunyi yang telah dihapuskan untuk mendapatkan tempoh masa yang tertentu daya pemotongan. Akhirnya, keputusan antara simulasi dan eksperimen menunjukkan bahawa pengoptimuman proses pemesinan boleh dilakukan dengan meramalkan daya pemotongan proses pengilangan dan juga memerhatikan pembentukan cip.

TABLE OF CONTENTS

	Page
SUPERVISORS'S DECLARATION	iii
STUDENT'S DECLARATION	iv
ACKNOWLEDGEMENT	v
ABSTRACT	vi
ABSTRAK	vii
TABLE OF CONTENTS	viii
LIST OF TABLES	xi
LIST OF FIGURES	xii
LIST OF SYMBOLS	xvii
LIST OF ABBREVIATIONS	xviii
CHAPTER 1 INTRODUCTION	
1.1 Introduction	1
1.2 Problem Statement	3
1.3 Objectives	3
1.4 Project Scope	4

CHAPTER 2 LITERATURE REVIEW

2.1	Introduction	5
2.2	Up Milling and Down Milling	5
2.3	Orthogonal and Oblique Cutting	6
2.4	Finite Element Analysis	8
	2.4.1 Approaches of Simulation	9
2.5	Cutting Parameter	13
	2.5.1 Influence on Cutting Speed	13
	2.5.2 Influence on Feed Rate	15
	2.5.3 Influence on Depth of Cut	20
2.6	Prediction of Cutting Force	21

CHAPTER 3 METHODOLOGY

3.1	Introduction	24
3.2	Milling Machine	26
3.3	Wire EDM Machine	27
3.4	Finite Element Analysis	29
3.5	Apparatus to Determine the Cutting Force	29
3.6	Workpiece Material	32
3.7	Methodology of Simulation	34

	x
3.8 Design of Experiment	68
CHAPTER 4 RESULT AND DISCUSSION	
4.1 Introduction	72
4.2 Result	72
4.2.1 Effects of Machining Parameters to Cutting Force	72
4.2.2 Cutting Force between Experimental and Theoretical Results	75
4.2.3 Stresses of Cutting Process	79
CHAPTER 5 CONCLUSION AND RECOMMENDATION	
5.1 Introduction	82
5.2 Conclusion	82
5.3 Recommendations	83
5.3.1 Cutting Force Measurement Experiment	83
5.3.2 Simulation of Side Milling Process	83
REFERENCE	84
APPENDICES	
A Gantt Chart of FYP 1	86
B Gantt Chart of FYP 2	87
C 600 SFM Cutting Speed From Dyno-Ware	88
D 700 SFM Cutting Speed From Dyno-Ware	89

LIST OF TABLES

Table No.	Title	Page
2.1	Material properties, geometry and composition of ST 44	16
2.2	Main cutting force and feed force	17
2.3	Cutting Temperature vs Change of Cutting Speed	18
2.4	Cutting Temperature vs Change of Cutting Depth	18
3.1	Performance of milling machine	27
3.2	Specifications of Wire EDM machine	28
3.3	Advantages and disadvantages of ABAQUS	29
3.4	Mechanical Properties of Aluminium 6061	33

LIST OF FIGURES

Figure No.	Title	Page
1.1	Schematic diagram of cutting force	2
1.2	Chip form classification	2
2.1	Up milling and down milling	6
2.2	Orthogonal cutting	7
2.3	Oblique cutting	8
2.4	Radial force and tangential force comparison between 2D and 3D model model	9
2.5	Eulerian (ALE) method	10
2.6	Eulerian (ALE) process model and example results	11
2.7	Reduction of yield stress and stiffness of plastic material after damage initiation	12
2.8	Lagrangian process model	12
2.9	Chip form classification	14
2.10	Chip morphologies at different cutting speed	14
2.11	Chip morphologies at different cutting speed	15
2.12	Main cutting force vs feed rate	19
2.13	Feed force vs feed rate	19
2.14	Chip morphologies with different feed rate	20

2.15	Chip sizes under different axial depth of cut	21
2.16	A Schematic Coordinate System Diagram	22
3.1	Flow chart	25
3.2	KE55 Vertical Machining Centre	26
3.3	Spark jump across the gap	27
3.4	Wire EDM machine	28
3.5	Three orthogonal direction	30
3.6	Multicomponent dynamometer	30
3.7	Dimension of dynamometer	31
3.8	4 channel charge amplifier	31
3.9	Aluminium block	32
3.10	Create raw material	34
3.11	Rectangular raw material	34
3.12	Dimension of raw material	35
3.13	Extrusion of raw material	35
3.14	Create cutting tool	36
3.15	Rectangular cutting tool	36
3.16	Dimension of cutting tool	37
3.17	Extrusion of cutting tool	37
3.18	Helix angle sketching	38
3.19	30 degree sketching	38
3.20	Rake angle	39
3.21	Clearance angle sketching	39
3.22	5 degree clearance angle	40

3.23	Extrusion of clearance angle	40
3.24	Material properties of Aluminium	41
3.25	Density of Aluminium	41
3.26	Elastic properties of Aluminium	42
3.27	Johnson Cook material properties	42
3.28	Johnson Cook damage failure model	43
3.29	Reference strain rate of Aluminium	43
3.30	Damage evolution of Aluminium	44
3.31	Material properties of high speed steel	44
3.32	Density of high speed steel	45
3.33	Elastic properties of high speed steel	45
3.34	Johnson Cook material properties	46
3.35	Johnson Cook material properties	46
3.36	Reference strain rate of high speed steel	47
3.37	Damage evolution of high speed steel	47
3.38	Aluminium section	48
3.39	Aluminium section	48
3.40	Steel section	49
3.41	Steel section	49
3.42	Create partition	50
3.43	Line of partition	50
3.44	Partition cell	51
3.45	Define it become Aluminium	51
3.46	Define both part become Aluminium	52
3.47	Define both part become Aluminium	52

3.48	Define steel material	53
3.49	Assembly workbench	53
3.50	Position the cutting tool and workpiece	54
3.51	Create step	54
3.52	Time period	55
3.53	Interaction properties	55
3.54	Friction coefficient between two materials	56
3.55	Interaction general contact	56
3.56	Attribute assignment	57
3.57	Create surface	57
3.58	Create rake surface	58
3.59	Create clearance surface	58
3.60	Create boundary condition	59
3.61	Fix the bottom surface of workpiece	59
3.62	Cutting tool boundary condition	60
3.63	Direction available of cutting tool	60
3.64	Distance of cutting tool moving	61
3.65	Time and amplitude	61
3.66	Global seed of the part	62
3.67	Edge local seed by using numbering method	62
3.68	Number of element for horizontal edge	63
3.69	Mesh and control the lower part	63
3.70	Explicit element type for element deletion	64
3.71	Mesh the part	64
3.72	After meshing	65

3.73	Global size of cutting tool	65
3.74	Mesh the part	66
3.75	Create the job	66
3.76	Status output for some failure and plasticity model	67
3.77	Job submission	67
3.78	Cutting workpiece material using wire cut	68
3.79	Complete workpiece material	69
3.80	Workpiece material on dynamometer	69
3.81	Dial test indicator	70
3.82	Experiment setup	70
3.83	12mm end mill	71
3.84	After the experiment	71
4.1	The chip formation of experiment	72
4.2	600 SFM metal cutting simulation	73
4.3	700 SFM metal cutting simulation	73
4.4	600 SFM radial force	75
4.5	700 SFM radial force	75
4.6	600 SFM tangential force	76
4.7	700 SFM tangential force	76
4.8	600 SFM axial force	77
4.9	700 SFM axial force	77
4.10	Stress distribution of 600 SFM	79
4.11	Stress distribution of 700 SFM	80
4.12	Simplified analytical model of the stress zone	80

LIST OF SYMBOLS

γ	Rake angle
α	Clearance angle
β	Wedge angle

LIST OF ABBREVIATIONS

Al	Aluminium
C	Carbon
CAD	Computer aided drafting
Fe	Iron
Mn	Manganese
P	Phosphorus
RPM	Revolution per minute
SFM	Square feet per minute
Si	Silicon
SKD	Alloy tool steel

CHAPTER 1

INTRODUCTION

1.1 INTRODUCTION

Machining is any of various processes in which a piece of raw material is used to cut and removes into desired shape and dimension by a controlled material removal process. It is widely used in the industry sector nowadays since its efficiency and effectiveness. There are three main principal machining processes which are drilling, turning and milling.

Milling is a material removal process, which can create a part that consists of many features by cutting away the unwanted material. The milling process commonly requires milling machine, cutting tool, workpiece and fixture. The workpiece is placed and fixed on the platform of milling machine. Whereas the cutting tool is inserted in the milling machine and rotates at high speeds. The workpiece is feeding with the cutting tools in which to remove the unwanted material to get desired shape.

Side milling process is important because it is widely used in industry because various shapes can be made with side milling process. The side milling is the process of production that the side milling cutter is cutting through the side of the workpiece. The cutting tool for side milling process made of variety of materials, carbide inserts are suitable for high production milling, high speed steel tool are used when special shape is needed, ceramics inserts are used for high speed milling and etc.

The quality of parts produced by side milling is related to the chip formation during the process. It is necessary to investigate the stresses and cutting forces generated during end milling. Thus, the different chip formation has their own mechanism was found to be the movement of cutting tool under different cutting conditions. The figure 1.2 shows the different types of chip formation(Wang et al. 2014). However, the cutting

forces can be calculated using several equations and the schematic diagram in figure 1.1 (Tsai et al. 2015).

$$\bar{F}_x = \bar{F}_{xc}a_c + F_{xe}$$

$$\bar{F}_y = \bar{F}_{yc}a_c + F_{ye}$$

$$\bar{F}_z = \bar{F}_{zc}a_c + F_{ze}$$

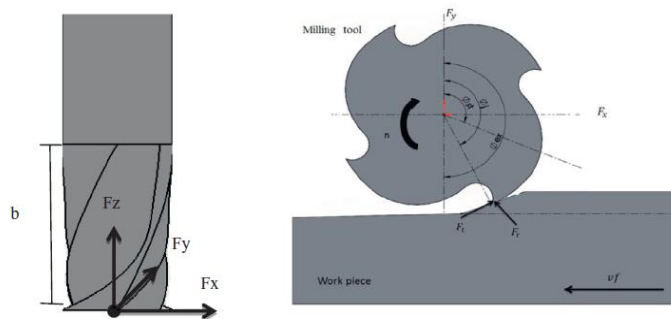


Figure 1.1: Schematic Diagram of Cutting Force

Source: Tsai et al. (2015)


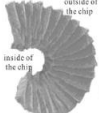
Curly form of chip	C-type	Continuous type
Upwards-curling		Chip length between 0.5 mm and 2 mm
Cross-curling		Chip length 2 mm or more

Figure 1.2: Chip Form Classification

Source: Wang et al. (2014)

Finite Element Analysis in machining processes is important to allow us to have comparison between theoretical and experimental results. It is a numerical technique used to finding the solutions to boundary value problems. It is used the division approach to focus the simpler parts from whole domain. It may get the representation from complex geometry which generated in end milling process.

Therefore, it is important to conduct this research to determine the best solution to determine the factors which will influence the chip formation during machining processes. Thus, ABAQUS is the tool appropriate to use in this research. ABAQUS could show that the stresses and forces generated during the machining process and the resulting effect towards chip formation. By comparing the results taken in ABAQUS, validating the factors which will influence the finishing parts is the best approach to improve machining processes.

1.2 PROBLEM STATEMENT

Side milling which is widely used in industry sectors has been emphasized to improve the quality of the part produced in terms of good tolerance, surface finish and forms. However, there are many aspects that could be improved in chip formation and machining factors in which would affect the product. Cutting forces are the main parameters which affect the surface finish of the machined products and tool life of the tool cutter. However, measurement of cutting forces is very expensive time taken to implement in a work shop. Therefore, the prediction and modelling of the cutting forces and machining mechanics would make it very ideal and easily applicable. In this project a finite element software ABAQUS will be used to prediction of cutting forces and stress distribution during the side milling process of aluminum.~~The failure of the setup of parameters would have produced the undesired shapes. There are many factors will effects the chip formation during machining processes. For instance, one of the factors is the tool life in which the tool wear would be one of the factor effects the chip formation.~~

1.3 OBJECTIVE

The objectives of this project are:

1. To determine the factors that influences the chip formation during machining process.
2. To predict the stresses and forces generated during machining process.
3. To validate the experimental and theoretical result of the machining process.

1.4 PROJECT SCOPE

The scope of this research is to investigate and validate the chip formation during and after the end mill process. Meanwhile, milling process has generated the stresses and cutting forces. The approach to investigate the chip formation in theoretical during end milling process by using FEM software which is ABAQUS. This software is able to analyze and calculate the modelled parts and shows the simulation process.

In the other hand, the investigation on the chip formation during end milling process will be done in the milling machine. Aluminum material will be needed to perform the end milling process. After both the experimental and theoretical result are taken, observation on the difference between the chip formations will be taken place.

CHAPTER 2

LITERATURE REVIEW

2.1 INTRODUCTION

This chapter explains the state of art of the machining mechanics related to the project. All the reviews are taken from the journals, articles, website and etc. The main purpose of this chapter is to make a comprehensive analysis of the research works from previous researchers. The chapter also examines the methods and mechanisms that affect the chip formation. Various parameters influence the chip formation, for example cutting forces, stress, feed rate, axial depth of cut and etc.

2.2 UP MILLING AND DOWN MILLING

There are two type of milling which are up milling and down milling. The result produced is totally different in several aspects. Having the deep understanding on both up milling and down milling will lead the good workpiece and also will extend the tool life. Figure 2.1 shows the up milling and down milling.

Up milling also define as conventional milling only produced small chips during the machining process. When the cutting process is carried on, chip thickness will be transformed from minimum to maximum until the end. The cutting forces generated also vary from zero to maximum.

Down milling also define as climb milling in which the direction of the feed of the workpiece is same with the cutter rotation. When the cutting process is carried on, chip thickness will be transformed from maximum to minimum until the end. Due to the direction of the feed of the workpiece is same with the cutter rotation, there is less friction will be occurred and thus results less heat energy generated between cutter and workpiece.

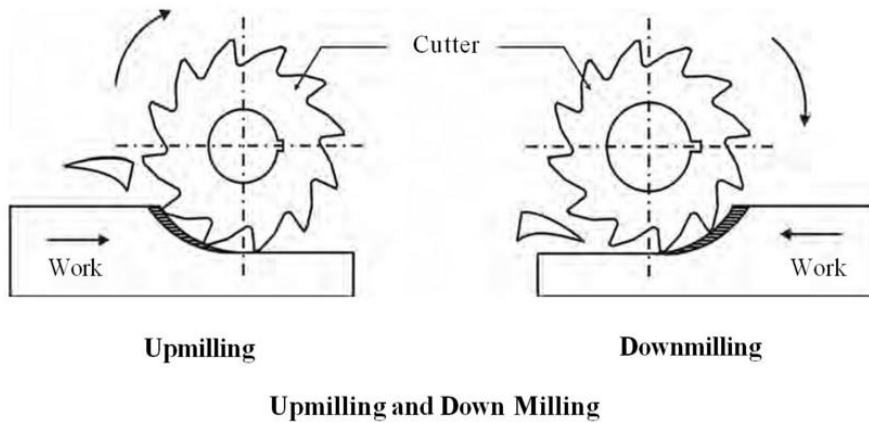


Figure 2.1: Up Milling and Down Milling

2.3 ORTHOGONAL AND OBLIQUE CUTTING

There are two different cutting schemes which is orthogonal and oblique cutting. In orthogonal cutting the cutting tool is perpendicular to the workpiece material when move along with it. By continue to remove the material of the workpiece, the cutting tool will back to the starting point or position and move downwards with certain of feed, f . There is the rake face and a line perpendicular to the workpiece surface which call rake angle, γ . The angle between the flank face and the workpiece material is clearance angle, α . Thus, the angle between rake angle and flank angle is wedge angle, β . Thus also, the sum of the three angles must be equal to 90° . Figure 2.2 and 2.3 shows the different between up milling and down milling.

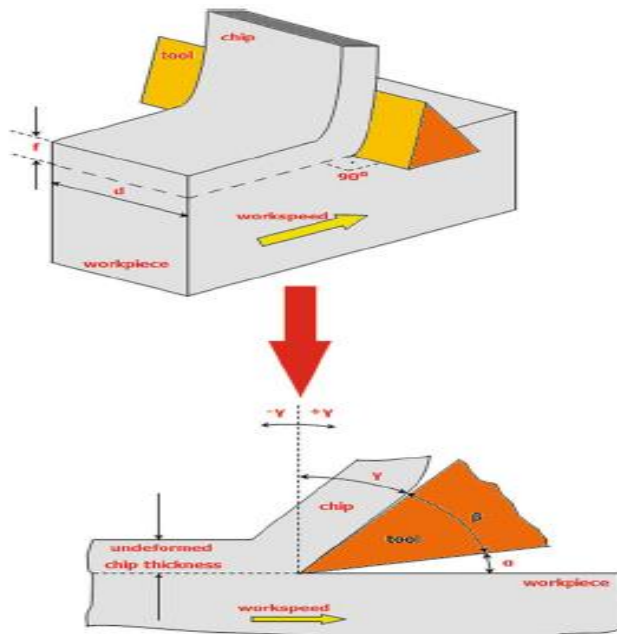


Figure 2.2: Orthogonal Cutting

Source: Markopoulos & Books24x7 Inc. (2013)

Oblique cutting is different with orthogonal cutting in term of the angle between the cutting tool and workpiece. The cutting tool is move along with the workpiece material more than or less than 90° (Markopoulos & Books24x7 Inc. 2013).

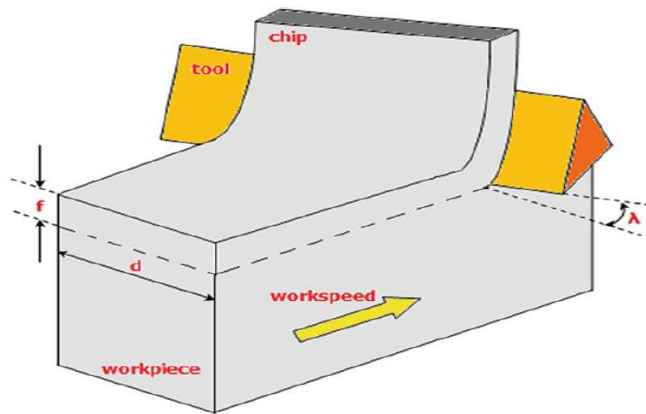


Figure 2.3: Oblique Cutting

Source: Markopoulos & Books24x7 Inc. (2013)

2.4 FINITE ELEMENT ANALYSIS

Finite element analysis is invented to analyze the process forming and design of the tools. Finite element analysis can be carried out with three steps, which is pre-processing, simulating and post-processing of the data taken from the machining process established (Constantin et al. n.d.). The rake face of the tools allows the chip deformed and sheared surface to move along with it (Margot et al. 2005). Finite element analysis allows researchers to do the prediction of the cutting forces, stresses, tool wear and temperature of the material removal process. Thus, with this method of designing the cutting tools, the best parameters and design can be determined. Finite element analysis has many advantages:

1. It solves the problem between the tool cutter and material.
2. Different material workpiece are used, the finite element curvilinear region can be determined (Constantin et al. n.d.).

Finite element analysis also is invented to analyze the chip formation mechanism and it allows researchers to study about how chip formation is happened and how it influences the quality of workpiece. Furthermore, the geometry can also be

simplified to 2 dimensional and 3 dimensional analyses. However, the analysis results was show slightly difference in radial(Schermann et al. 2006).

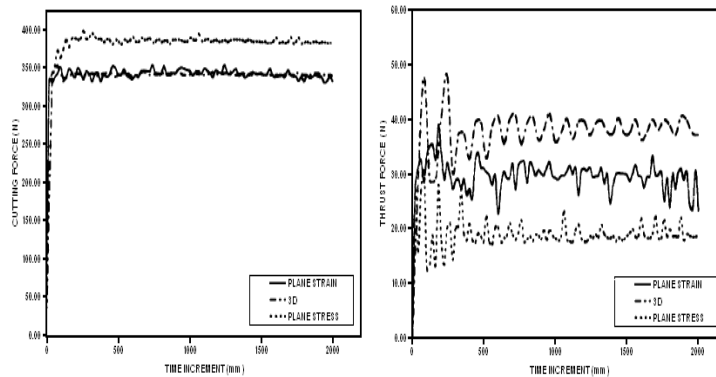


Figure 2.4: Radial force and tangential force comparison between 2D and 3D models

Source: (Adetoro & Wen n.d.)

2.4.1 Approaches of Simulation

Finite element analysis basically provides two re-meshing approaches to accomplish the simulation for machining processes, which is Eulerian and Lagrangian approach(Schermann et al. 2006). The Eulerian is the method to allow the workpiece flow through the mesh generated. The flow of the material is independent to the mesh nodes inside the workpiece. Furthermore, the Eulerian act as the outflow of the workpiece is tangential to the surface of the workpiece. The Eulerian region inside the workpiece is flow along with the direction of the inflow. The frictional contact shear stresses occurred on the surface of the workpiece is transferred to the material flow. Eulerian method is the most effective method for detailed studies in chip formation(Schermann et al. 2006). It implies the shape of chip formation, shear zone angle, and the contact conditions of the cutting tools and workpiece is the priority to know; either it is derived from experiment or prediction. However, derivation for strains

from the integration of strain rates along stream lines(Markopoulos & Books24x7 Inc. 2013). The figure 2.5 below shows the Eulerian (ALE) process model during the machining process.

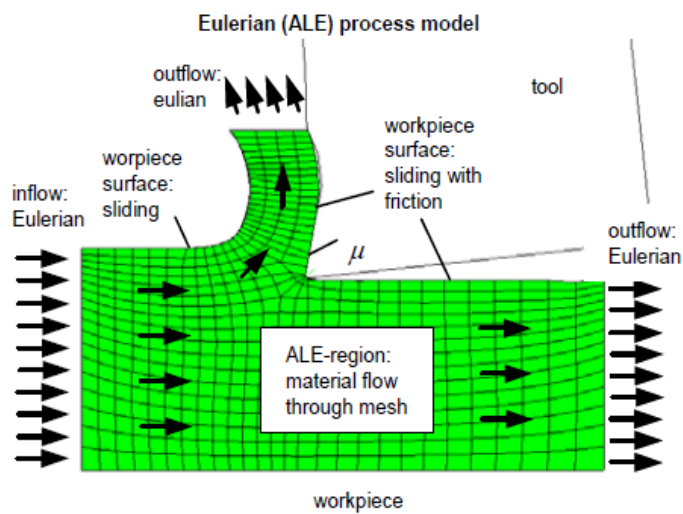


Figure 2.5: Eulerian (ALE) Method

Source: Schermann et al. (2006)

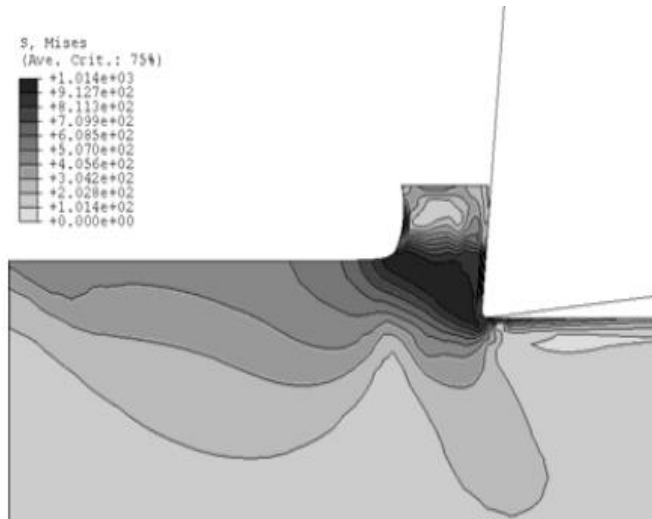


Figure 2.6: Eulerian (ALE) process model and example results

Source: Schermann et al. (2006)

Lagrangian is the method that the movement of workpiece is dependent to the mesh nodes inside the workpiece. In order to separate the material flow with the tool tips under optimize situation, elimination of elements according to appropriate failure criteria must be done. It is done by reduce the yield stress and stiffness of plastic material after the damage has been initiated with damage variable, D . The figure below shows Lagrangian process model. Besides that, ANSYS provides the various failure modes with and without damage initiation and damage evolution before delete the elements. Calibration of failure and damage models must be careful(Schermann et al. 2006). Thereby, several modes that relate on strain, strain rate and also temperature can be applied on material workpiece(Markopoulos & Books24x7 Inc. 2013).

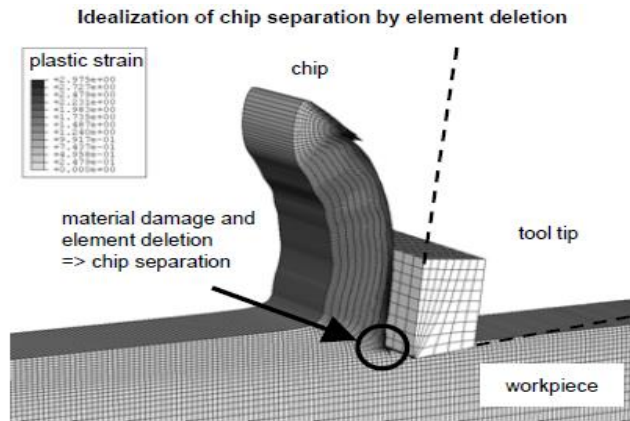


Figure 2.7: Reduction of yield stress and stiffness of plastic material after damage initiation

Source: Schermann et al. (2006)

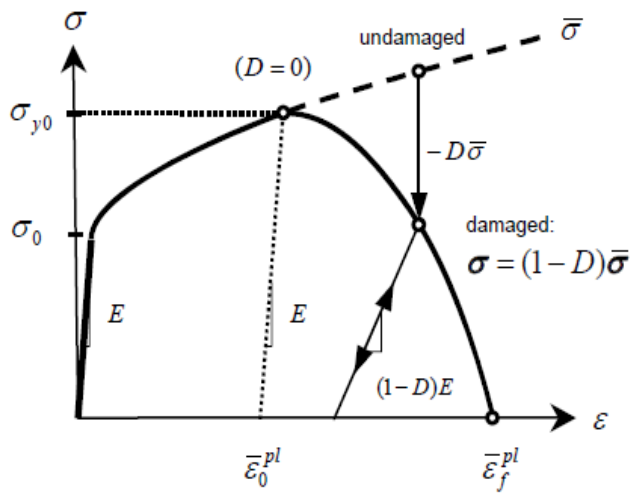


Figure 2.8: Lagrangian Process Model

Source: Schermann et al. (2006)

2.5 CUTTING PARAMETERS

Cutting parameters seem important in the prediction of cutting force, because it will manipulate the chip formation directly in machining processes. Those parameters are feed rate, axial depth of cut, and cutting speed.

2.5.1 Influence of Cutting Speed

SKD 11 (62 HRC) and S136 (51HRC) are used to observe the morphological changes of chips under various cutting conditions. Both of the materials have different hardness. The results show that when the cutting speed was slow, chip formation will be in continuous belt with regular deformations. While when the cutting speed increases, the chip morphology will transformed into saw-tooth, and the shape of the chip is into high deformation concentration shear band, uniform interval. A shining white layer was present at the bottom of the chip. The chip formation can be observed in figure 2.10 and 2.11. The size of the chip also changed with cutting speed, it can be seen in the figure 2.9 and 2.10. When the cutting speed increases, the velocity of the metal flow also increased, thus the thickness of the saw-tooth chip equivalent decreases. Other than that, the distance between the saw-tooth also increased, separation trend of saw-tooth deepened, degree of deformation increased(Şeker et al. 2004).

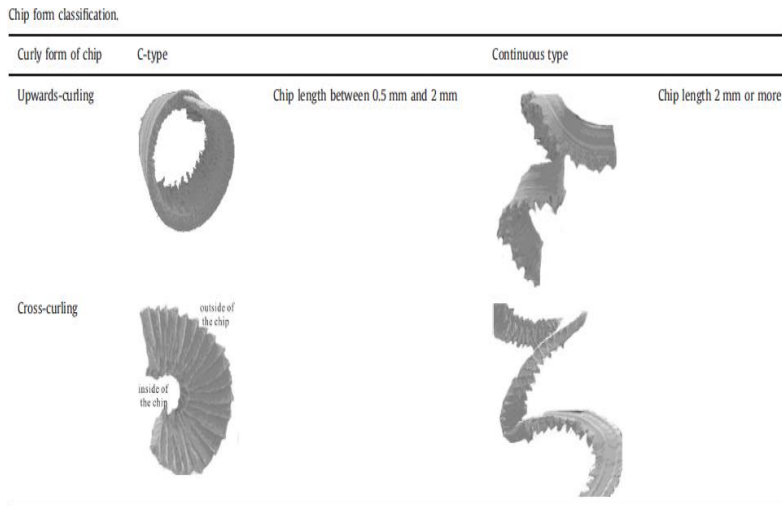


Figure 2.9: Chip form classification

Source: (Wang et al. 2014)

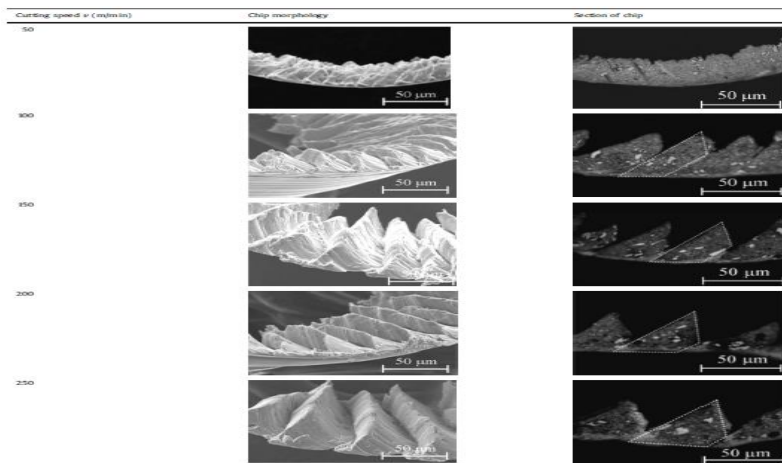


Figure 2.10: Chip morphologies at different cutting speed

Source: Wang et al. (2014)

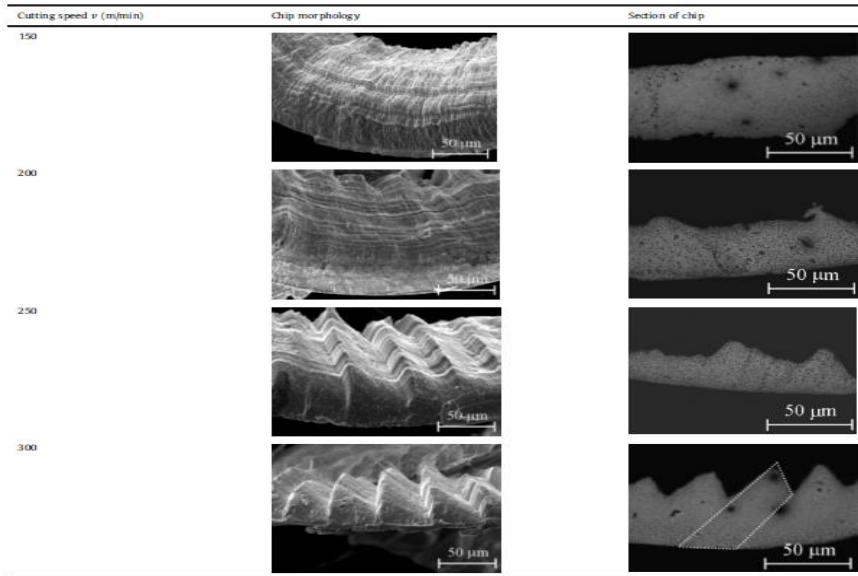


Figure 2.11: Chip morphologies at different cutting speed

Source: Wang et al. (2014)

2.5.2 Influence of feed rate

In the analysis of influence of feed rate on the cutting force in machining process, ST 44 was chosen as the workpiece materials. ST 44 will first mill to remove the impurities of the surfaces. The properties, geometry and composition of ST 44 were shown in Table 2.1(Şeker et al. 2004).

Workpiece Material	St 44
Chemical Composition (%)	
C	0.16
Si	0.23
Mn	0.92
P	0.014
S	0.009
Al	0.036
Fe	Balance
Dimensions (mm)	90 x 90 x 32
K_{II} (N/mm ²)	1780
m	0.17

Table 2.1: Material properties, geometry and composition of ST 44
(Şeker et al. 2004)

The entire group shows that the main cutting forces and feed forces increase with the increasing feed rate. The axial depth of cut and cutting speed help constant in each group in order to get accurate result. The feed rate shows the obviously effect on main cutting forces rather than the feed forces. The main cutting force was calibrated as the highest forces. During the machining process, the friction forces and tool geometry between the cutting tool and workpiece will affect the existence of the feed forces. Thus, the increasing cutting velocity will result the cutting forces increased with also increased the friction force. The results can be seen in Table 2.2 and Figure 2.12 and 2.13(Şeker et al. 2004).

Furthermore, the color of the chip has the strong relationship with the cutting speed and feed rate. The higher the cutting speed and feed rate, the darker the color of the chip. This indicates that the level of oxidation leads to higher temperature. Thus, the optimum cutting parameters is not as high as possible because the level of oxidation means the tool wear will be increase monotonously, this will results the surface finish of the workpiece are adversely affected. Table 2.3 and 2.4 shows the results of chip color with varying the cutting speed(Ning et al. 2001).

Table 2.2: Main cutting force and feed force

Source: Şeker et al. (2004)

Group number	Experiment number	Mean deflection for F_C	F_C (N)	Mean deflection for F_f	F_f
1	1	0.1851	63.33	0.07162	7.72
	2	0.2883	93.77	0.0753	8.06
	3	0.4520	142.04	0.08175	8.64
	4	0.5310	165.35	0.08605	9.03
2	5	0.1386	49.62	0.07527	8.05
	6	0.2421	80.14	0.07737	8.24
	7	0.3561	113.77	0.08402	8.52
	8	0.4787	149.94	0.08182	8.65
3	9	0.0441	21.75	0.0387	4.73
	10	0.0938	36.42	0.0478	5.56
	11	0.1612	56.30	0.0682	7.41
	12	0.1878	64.12	0.07982	8.47
4	13	0.0319	18.16	0.04547	5.35
	14	0.0634	27.45	0.05857	6.54
	15	0.1697	58.81	0.07547	8.07
	16	0.1988	67.37	0.08152	8.62

Table 2.3: Cutting Temperature vs Change of Cutting Speed

Source: Ning et al. (2001)

Rpm (k)	A_p (mm)	Chip Color	Temperature (°C)
30	0.5	Dark Blue + Green	>1000
25	0.5	Dark Blue	960 – 1000
24	0.5	Blue + Purple	920 – 960
22	0.5	Blue + Brown	860 – 920
20	0.5	Brown	820 – 880
18	0.5	Light Brown	800 - 840

Table 2.4: Cutting Temperature vs Change of Cutting Depth

Source: Ning et al. (2001)

Rpm (k)	A_p (mm)	Chip Color	Temperature (°C)
20	0.7	Dark Blue + Green	>1000
20	0.6	Dark Blue	960 – 1000
20	0.5	Blue + Purple	920 – 960
20	0.4	Blue + Brown	860 – 920
20	0.3	Brown	820 – 880
20	0.2	Light Brown	800 - 840

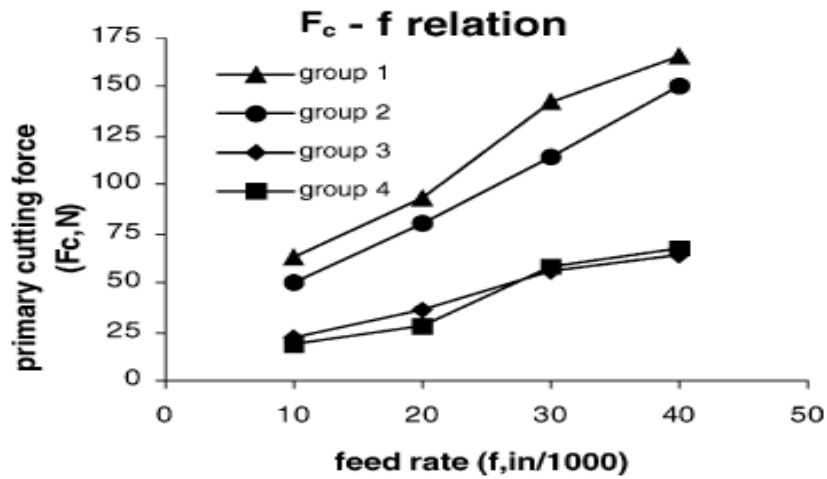


Figure 2.12: Main cutting force vs feed rate

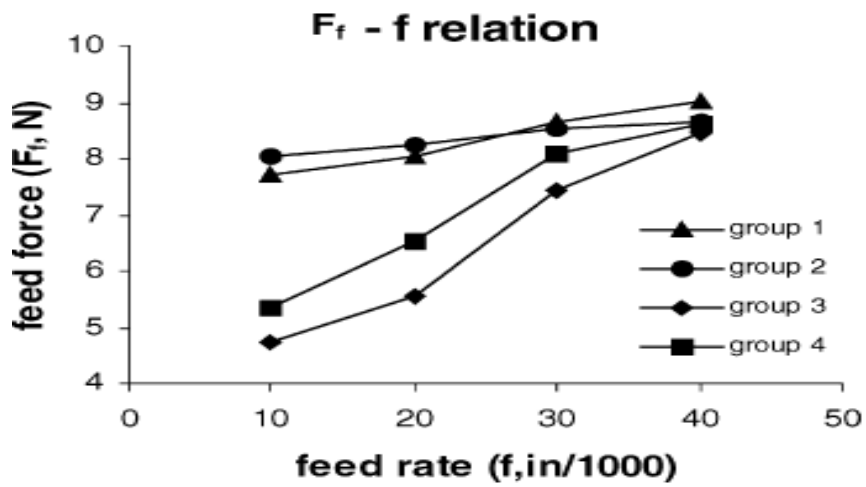


Figure 2.13: Feed force vs feed rate

Source: Şeker et al. (2004)

2.5.3 Influence on axial depth of cut

SKD 11 (62 HRC) was chosen as workpiece material to analyze the influence of axial depth of cut on the change in chip morphology during machining process. It is subjected under different axial depth of cut condition, and different chip size with different axial depth of cut. When the axial depth of cut is small, the shape of the chip will be in continuous belt with homogeneous deformation, but however the chip thickness began to appear the fluctuation. While when the axial depth of cut is increased, the saw-tooth chip began to generated, the width cutting increased. After that, the saw-tooth chip thickness increased and the chip thickness decreased gradually in which located in the local shear deformation zone. Thereby, the saw-tooth distance would increase regularly with the increasing axial depth of cut(Wang et al. 2014). Figure 2.14 and 2.15 shows the chip morphologies with different feed rate and chip sizes under different axial depths of cut respectively.

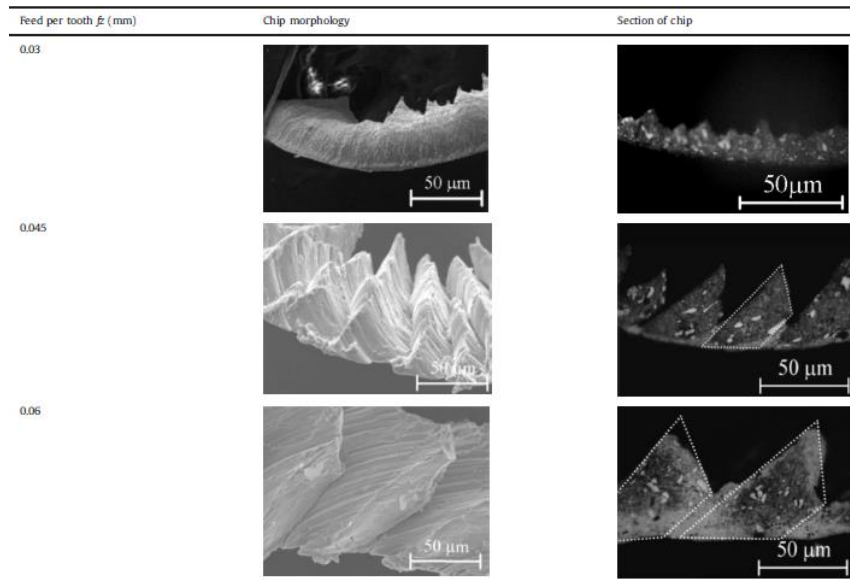


Figure 2.14: Chip morphologies with different feed rate

Source: Wang et al. (2014)

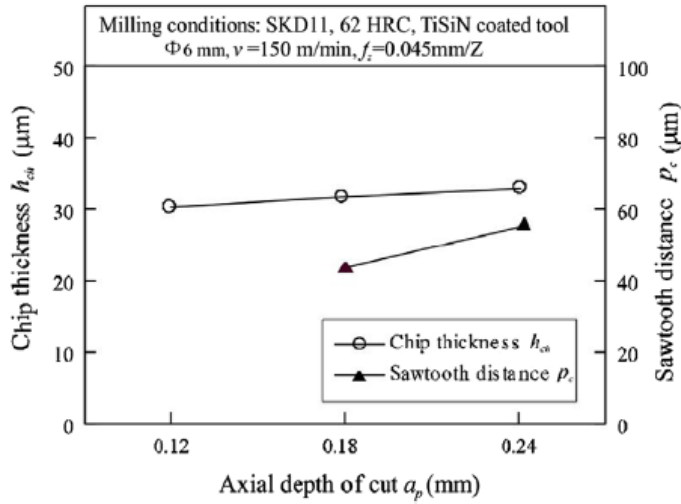


Figure 2.15: Chip sizes under different axial depths of cut

Source: Wang et al. (2014)

2.6 Prediction of Cutting Force

Aluminum 6060-T6 was chosen as workpiece material to analyze the prediction of cutting force. Altintas method was the method used in this analysis. The investigation of the influence of feed per tooth and tooth diameter on the cutting force coefficient and cutting force is also taken in this study.

The Altintas model was ignoring the tool run out and evaluates the force. The force component can be evaluated using the equation below:

$$dF_t = K_{tc} a_c db + K_{te} dl$$

$$dF_r = K_{rc} a_c db + K_{re} dl$$

$$dF_a = K_{ac} a_c db + K_{ae} dl$$

In the equation, dF_t , dF_r , dF_a represented the cutting force element in tangential, radial and axial respectively. K_{tc} , K_{rc} , K_{ac} represented the tangential, radial, and axial cutting

force coefficients. Further, db , dl , a_c represented the chip width, length for an infinitesimal section of the chip and cutting thickness respectively. K_{te} , K_{re} , K_{ae} represented tangential, radial and axial edge force coefficients. The coordinate system diagram is set up as shown in figure 2.16(Tsai et al. 2015).

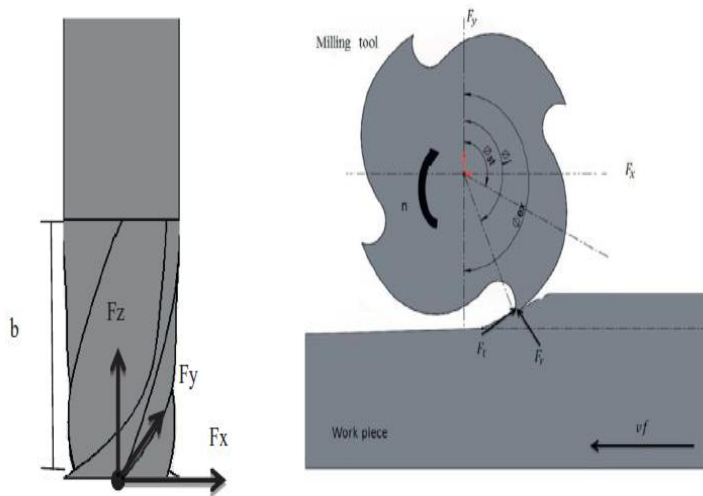


Figure 2.16: A Schematic Coordinate System Diagram

Source: Tsai et al. (2015)

The direction of the X-axis and feed are opposite each other. Y-axis is in normal direction. Z-axis is the direction from cutting tool point to spindle. The cutting force in X, Y and Z direction was obtained by using the derivation as below:

$$F_x = -\left[\frac{Nba_c}{8\pi} [K_{tc} \cos 2\varphi - K_{rc} (2\varphi - \sin 2\varphi)]\right] + Nb/2\pi [-K_{te} \sin \varphi + K_{re} \cos \varphi]_{\varphi_{st}}^{\varphi_{ex}}$$

$$F_y = \left[\frac{Nba_c}{8\pi} [K_{tc} (2\varphi - \sin 2\varphi) - K_{rc} \cos 2\varphi] - \frac{Nb}{2\pi} [K_{te} \cos \varphi + K_{re} \sin \varphi]\right]_{\varphi_{st}}^{\varphi_{ex}}$$

$$F_z = \left[\frac{Nb}{8\pi} [-K_{ac} a_c \cos \varphi + K_{ac} \varphi] \right]_{\varphi_{st}}^{\varphi_{ex}}$$

Where φ is represented as contact angle; N is the tool teeth; b is the axial depth of cut. Where φ_{st} and φ_{ex} are the entry and exit points. Thus the value is 0 and 180 respectively. Since the cutter eccentricity would be influenced during the measurement, thus the total cutting force for each revolution was measure, and then the results will be taken by divided the tool teeth number(Tsai et al. 2015). Substituting the phase angle in the equation will obtained the equations below:

$$\overline{F}_x = \frac{Nb}{4} K_{rc} a_c + \frac{Nb}{\pi} K_{re}$$

$$\overline{F}_y = \frac{Nb}{4} K_{tc} a_c + \frac{Nb}{\pi} K_{te}$$

$$\overline{F}_z = \frac{Nb}{\pi} K_{ac} a_c + \frac{Nb}{2} K_{ae}$$

And the equations can be written as:

$$\overline{F}_x = \overline{F}_{xc} a_c + F_{xe}$$

$$\overline{F}_y = \overline{F}_{yc} a_c + F_{ye}$$

$$\overline{F}_z = \overline{F}_{zc} a_c + F_{ze}$$

Also, the cutting force coefficient can be expressed as below(Tsai et al. 2015):

$$K_{tc} = \frac{4\overline{F}_{yc}}{Nb} \quad K_{te} = \frac{\pi\overline{F}_{ye}}{Nb}$$

$$K_{rc} = \frac{4\overline{F}_{xc}}{Nb} \quad K_{re} = \frac{\pi\overline{F}_{xe}}{Nb}$$

$$K_{ac} = \frac{\pi\overline{F}_{zc}}{Nb} \quad K_{ae} = \frac{2\overline{F}_{ze}}{Nb}$$

CHAPTER 3

METHODOLOGY

3.1 INTRODUCTION

This chapter will explain the detail methods and approaches to achieve the objectives of this project. It is stated in detail about the material, apparatus, and computer software that will be used in this project. The flowchart as shown in Figure 3.1 below is the overview of the methods that will be used in the project.

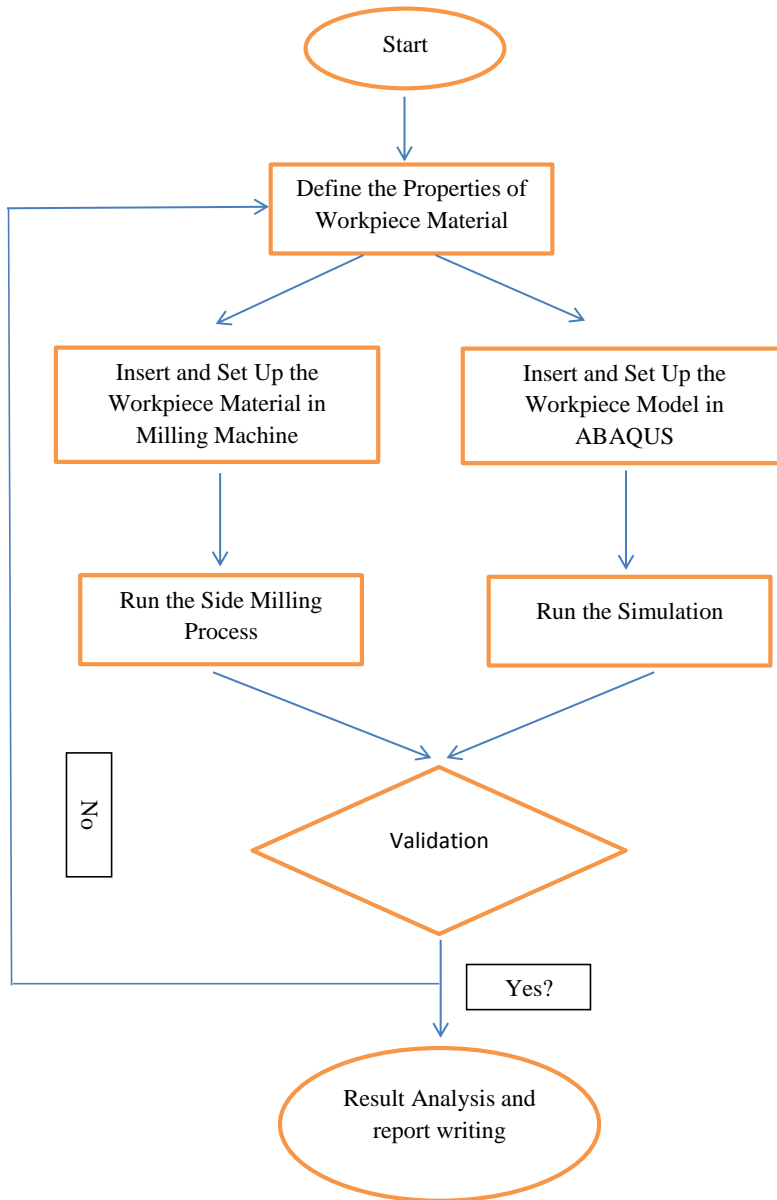


Figure 3.1: Flow Chart

3.2 MILLING MACHINE

Milling machine is used to shape the workpiece material in order to obtain the desired dimension products by eliminating excess material. Milling machine can be used to operate many material removal processes such as slot cutting, threading, drilling, pocketing and etc. Milling machine basically can be used to cut of wide range metals from aluminum to stainless steel. The machine can be set to operate at a faster or slower speed in which depends on the materials to be cut. Soft material usually will operate under higher speed while hard material will operate under slower speed.

The model that will be used in this project is KE55 Vertical Machining Centre. The performance of this milling machine is shown in Table 3.1. First of all, the dimensions of the Aluminum 6061 is not appropriate to use for experiment because the dynamometer has the limitation



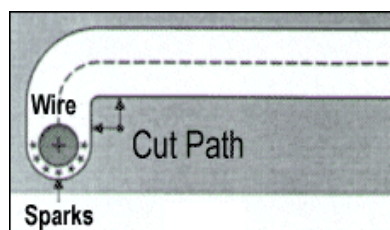
Figure 3.2: KE55 Vertical Machining Centre

Table 3.1: Performance of Milling Machine

Cutting Tool	Ø 80 Face Mill and 45° Entry Angle	Ø25 Drill Insert Type	Ø20Ru.E.M.H. s.s.co
Speed (rpm)	1270	1300	400
Cutting Speed (m/min)	300	102	25
Feed (mm/min)	1140	200	100
Depth of cut (mm)	3.2		20
Width of cut (mm)	50	25	20
Metal Removal Rate (cm ³ /min)	182	98.2	40

3.3 WIRE EDM MACHINE

Wire Electrical Discharge Machine is also known as a manufacturing process in which a desired shape is obtained using the method of electrical discharges- sparks. The desired dimension and shape will be shaped by removing the material from workpiece with a series of rapidly recurring current discharges between two electrodes. Thus, as the spark created from EDM machine will jump across the gap as shown in Figure 3.3. However, to stop and prevent the short out of the sparking process, non-conductive fluid will be applied, then the dielectric will remove the materials, which the process continues.

**Figure 3.3:** Spark jump across the gap

The model of Wire EDM Machine we have used in this project is Sodick VZ 300L as shown in Figure 3.4. Furthermore Table 3.2 shows the specifications of the Wire EDM Machine.



Figure 3.4: Wire EDM Machine

Table 3.2: Specifications of Wire EDM Machine

X - Axis Travel	13.78" (350 mm)
Y - Axis Travel	9.84" (250 mm)
Z - Axis Travel	8.66" (220 mm)
U, V Axis Travel	3.15" x 3.15" (80 x 80 mm)
Wire Diameter Range (min ~ max)	0.004" ~ 0.012" (0.10 ~ 0.30 mm)
Work Tank Dimensions (W x D)	31.89" x 25.59" (810 x 650 mm)
Maximum Workpiece Weight	1,102 lbs (500 kg)
Distance From Floor to Table Top	35.43" (900 mm)
Machine Tool Dimensions	74.61" x 85.83" x 77.17" (1,895 x 2,180 x 1,960 mm)
Machine Weight	5,280 lbs (2,400 kg)

3.4 FINITE ELEMENT ANALYSIS SOFTWARE

This project requires simulation software to determine the stresses and cutting forces generated in machining process. The software will be used in this project is Abaqus. Abaqus can be used to simulate many interactions in all aspects which are physics, structural, vibration, fluid dynamics, heat transfer and also electromagnetic for engineers. Thus, Abaqus capable of simulating the test and working conditions, which is beneficial to us test in virtual environments before manufacturing the finished or prototyping products. Furthermore, it also can be used to investigate and determine the weak parts, forecasting the problems might be appeared in the virtual environment. ‘Preprocessing’ the geometry can be done by import the CAD part into Abaqus to analyze purpose. There are many advantages of Abaqus over than the others Finite Element Analysis Software as shown in Table 3.3 (Constantin et al. n.d.).

Table 3.3: Advantages and disadvantages of ABAQUS

	Advantages	Disadvantages
Abaqus	<ol style="list-style-type: none"> 1. Clear detail 2. Design the workpiece, tool manually, free modelling. 3. Configuration of the materials 4. Finer meshing 	<ol style="list-style-type: none"> 1. Has no support for any materials. 2. Plenty of the parameters setup of the simulation.

3.5 APPARATUS TO DETERMINE THE CUTTING FORCE

The apparatus to use to measure the cutting forces and torques during high speed milling machine in this project is Multicomponent Dynamometer 9257B. This sensor is used to measure the quasi-static and dynamic force component in three orthogonal directions, F_x , F_y , and F_z .

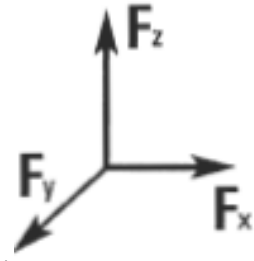


Figure 3.5: Three Orthogonal Directions

Multicomponent Dynamometer is designed to consist of four three component force sensors located under high preload between a baseplate and top plate. The sensors have three pairs of quartz plates, these pairs of quartz sensitive to different load in which one sensor only detect pressure in the z direction, while the other two are responding to shear stress in the x and y directions respectively. The force measurements are all considered without displacement.



Figure 3.6: Multicomponent Dynamometer

Furthermore, all of the sensors are well ground-insulated. Thus, ground loop problems can be completely eliminated. Moreover, the dynamometer is waterproof from cooling agent and protected against the rust. There is another special thermal isolation coating integrated in the top plate which prevent the dynamometer decrease the sensitivity towards influences of temperature. The figures 3.7 shows that the dimensions of the dynamometer(Group 2009).

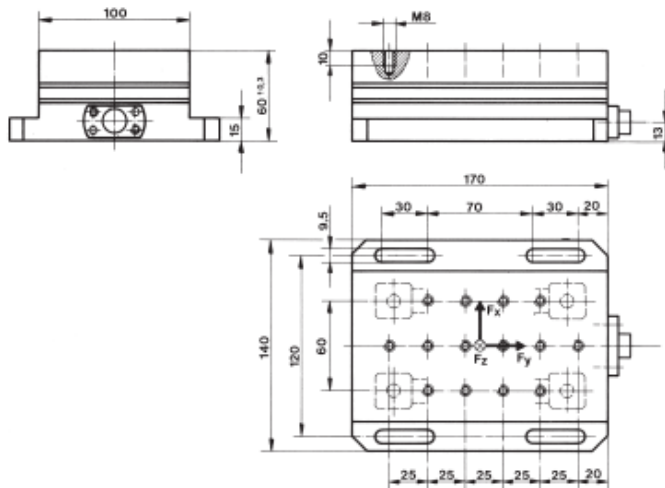


Figure 3.7: Dimension of Dynamometer

Next, the amplifier will be used in this project is 3 Component Force Measurement F_x , F_y , F_z with 4- Channel Charge Amplifier Type 5070 Ax01xx. Figures 3.8 shows the diagram of amplifier.



Figure 3.8: 4 Channel Charge Amplifier

Last but not least, the software will be used to in this project is Dyno-ware. This software is the data acquisition software of choice for cutting force measurement. This software can evaluate all the measured data which received from signal amplifiers produce from other manufacturers.

3.6 WORKPIECE MATERIAL

The workpiece material will be used in this project is aluminum. Aluminum is a kind of metallic element and the third most plentiful of all elements in the Earth layer. Mining the aluminum ore or bauxite is the first step to obtain aluminum. Then it will chemically refine to produce alumina product through the Bayer process. Electrolyte process will be carrying out to refine the alumina to pure metal.



Figure 3.9: Aluminum Block

However, there are many type of aluminum 7005, 7050, 7075 and etc. In this project, the raw materials will use in experiment is Aluminum 6061. The table 3.4 shows the mechanical properties of Aluminum 6061. The density of Aluminum 6061 is 2700 kg/m^3 .

Table 3.4: Mechanical Properties of Aluminium 6061

Hardness, Brinell	95
Hardness, Knoop	120
Hardness, Rockwell A	40
Hardness, Rockwell B	60
Hardness, Vickers	107
Ultimate Tensile Strength	310MPa
Tensile Yield Strength	276MPa
Elongation at Break	12%
Elongation at Break	17%
Modulus of Elasticity	70Gpa
Notched Tensile Strength	324MPa
Ultimate Bearing Strength	607MPa
Bearing Yield Strength	386MPa
Poisson's Ratio	0.33
Fatigue Strength	96.5MPa
Fracture Toughness	29MPa-m ^{1/2}
Machinability	50%
Shear Modulus	26GPa
Shear Strength	207MPa

3.7 METHODOLOGY OF SIMULATION

1. Create raw material, the type of raw material is deformable and the base feature is solid form.

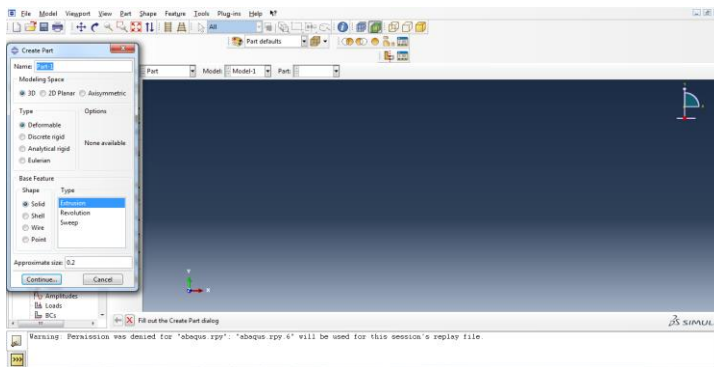


Figure 3.10: Create raw material

2. Draw the rectangular as raw material.

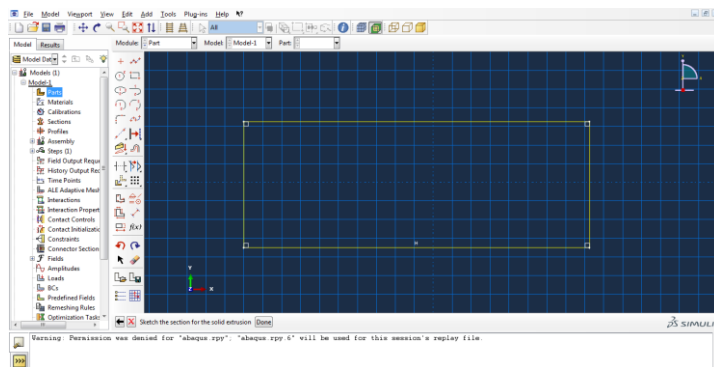


Figure 3.11: Rectangular raw material

3. Set the dimensions of raw material

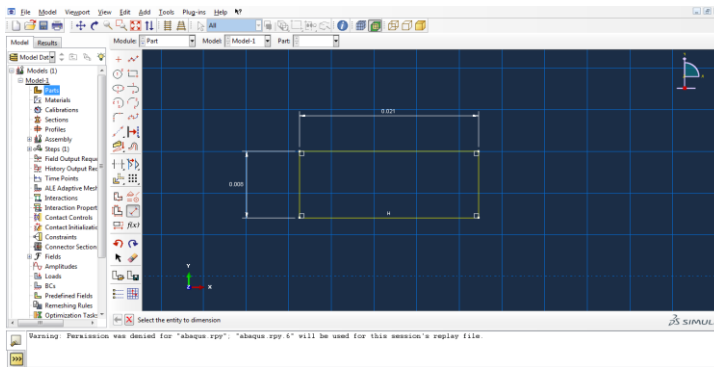


Figure 3.12: Dimension of raw material

4. Set the value of extrusion which is the depth of the raw material.

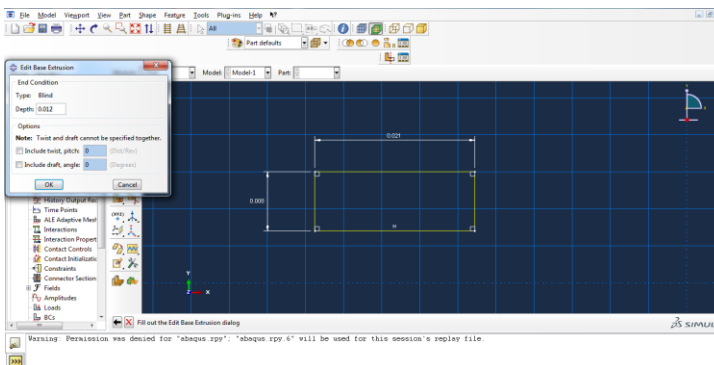


Figure 3.13: Extrusion of raw material

5. Create the cutting tool, the type is deformable and the base feature is solid.

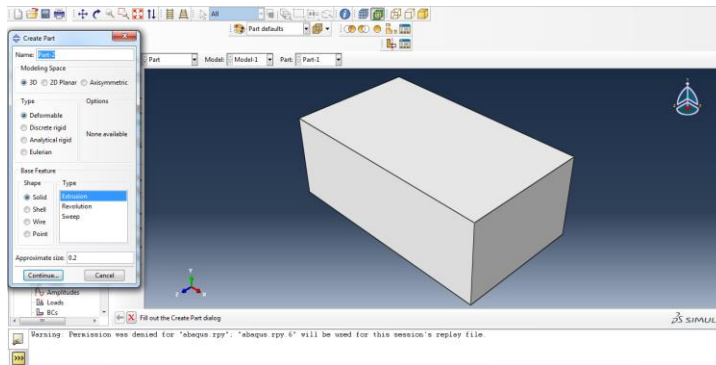


Figure 3.14: Create cutting tool

6. Draw the rectangular as cutting tool.

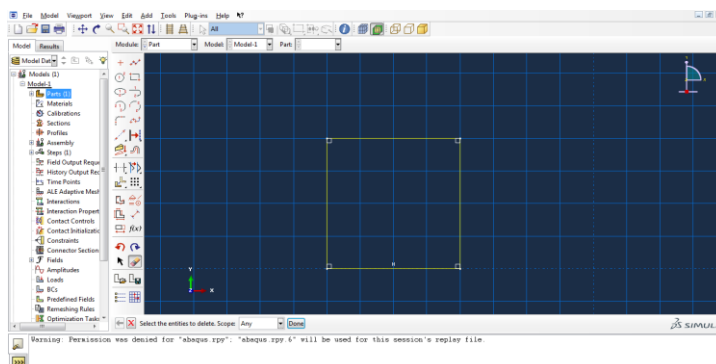


Figure 3.15: Rectangular cutting tool

7. Set the dimension of cutting tool.

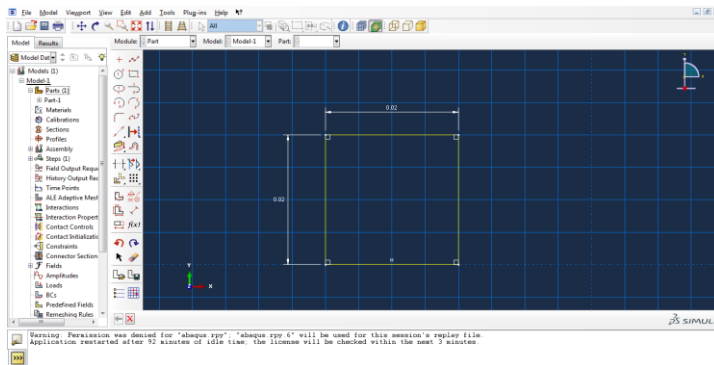


Figure 3.16: Dimension of cutting tool

8. Set the value of extrusion which is the width of cutting tool.

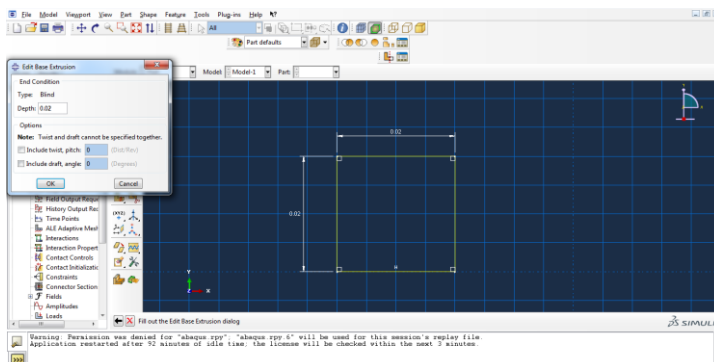


Figure 3.17: Extrusion of cutting tool

9. Use the extrude cut to produce the helix angle. Select the surface to sketch the angle.

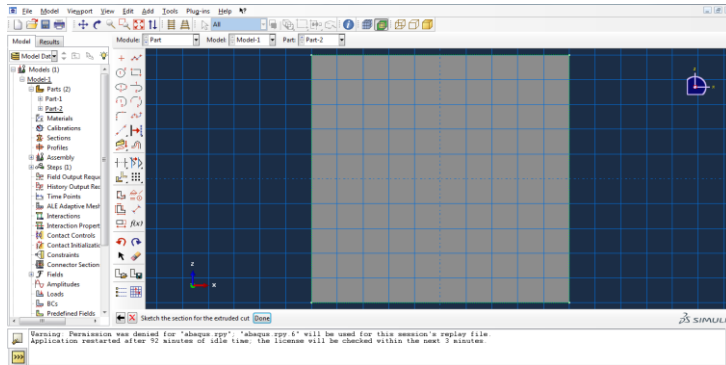


Figure 3.18: Helix angle sketching

10. Sketch the 30° drawing, the helix angle of cutting too is 30°

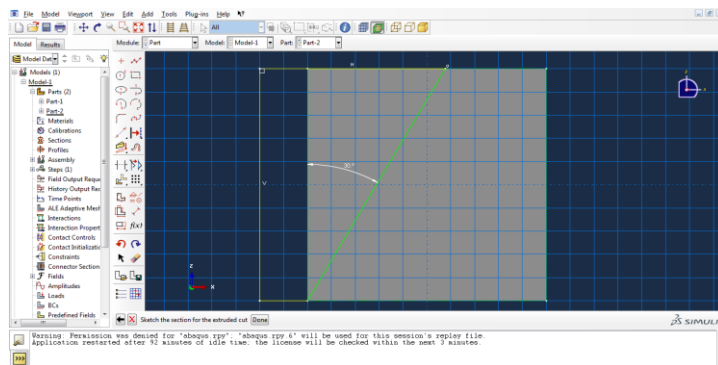


Figure 3.19: 30 degree sketching

11. Draft the angle to become as rake angle, the rake angle is 15°

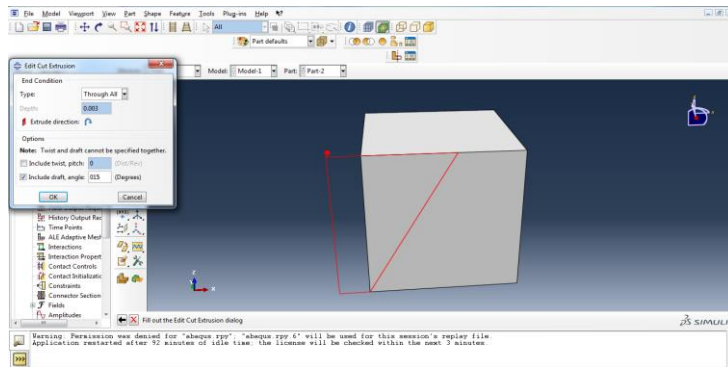


Figure 3.20: Rake angle

12. Use the extrude cut to produce the clearance angle. Select the surface to sketch the angle.

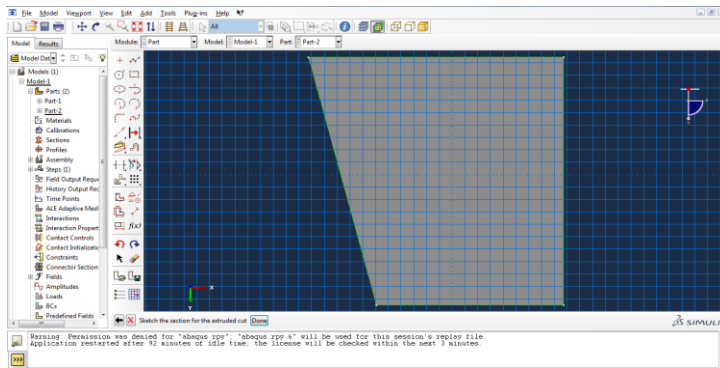


Figure 3.21: Clearance angle sketching

13. Sketch the 5° drawing.

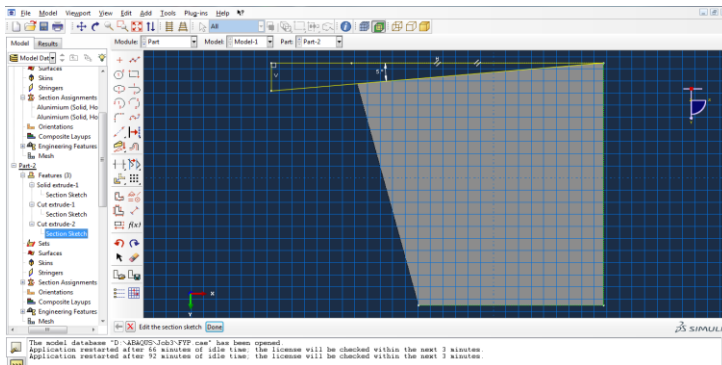


Figure 3.22: 5 degree clearance angle

14. Cut the extrusion without any draft and twist to create clearance angle.

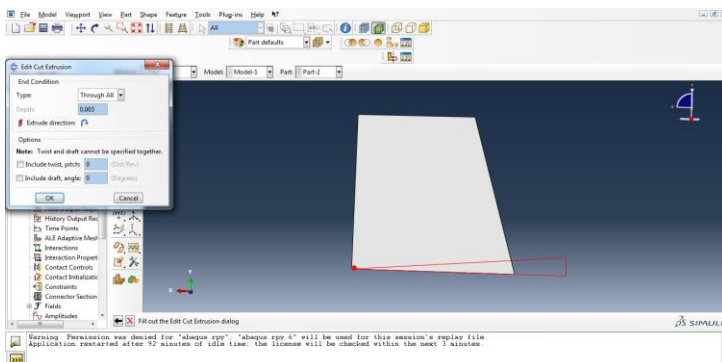


Figure 3.23: Extrusion of clearance angle

15. Apply the material properties of Aluminium.

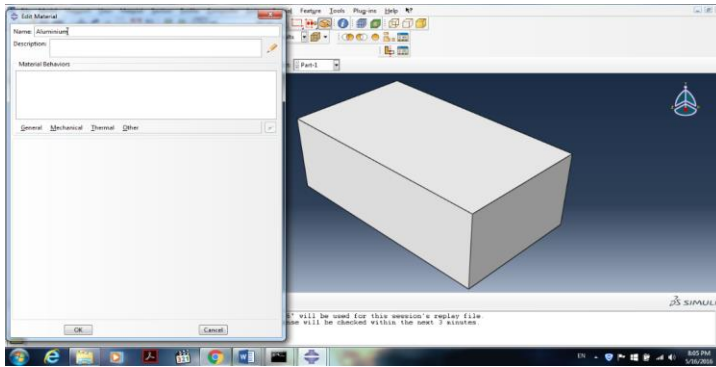


Figure 3.24: Material properties of Aluminium

16. Fill in the value of density of Aluminium, the density is 2700 kg/m^3 .

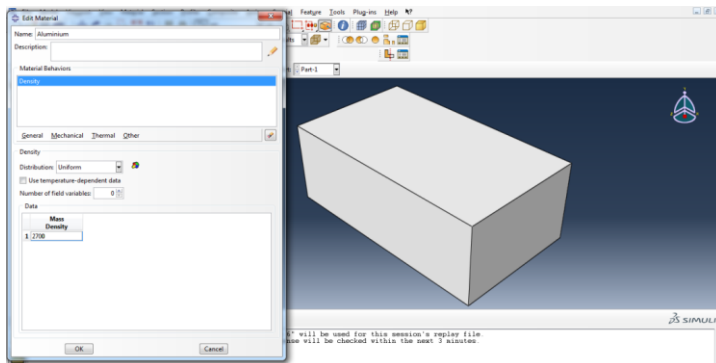


Figure 3.25: Density of Aluminium

17. Fill in the value of Young's Modulus and Poisson Ratio. The young modulus is 70 GPa and Poisson's ratio is 0.33.

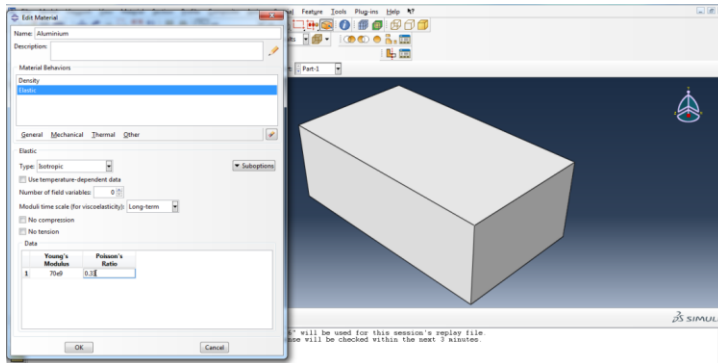


Figure 3.26: Elastic properties of Aluminium

18. Fill in the Plastic Properties by using Johnson Cook Model.

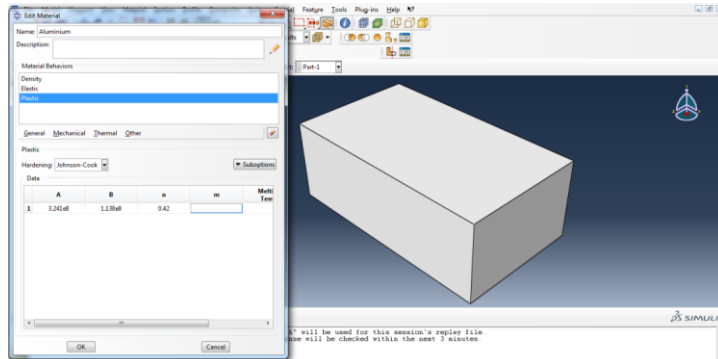


Figure 3.27: Johnson Cook material properties

19. Fill in the value of Johnson Cook Damage Failure Model.

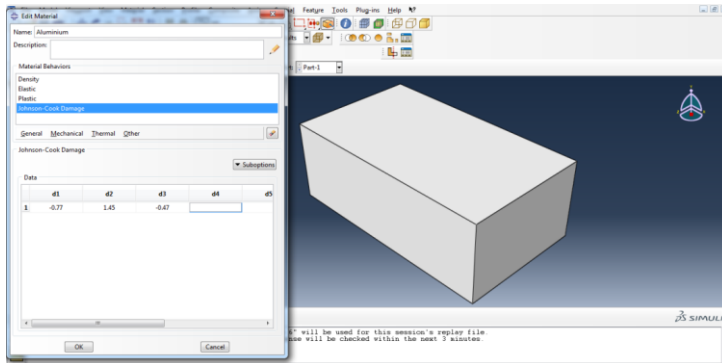


Figure 3.28: Johnson Cook Damage Failure Model

20. Fill in the value of Reference Strain Rate.

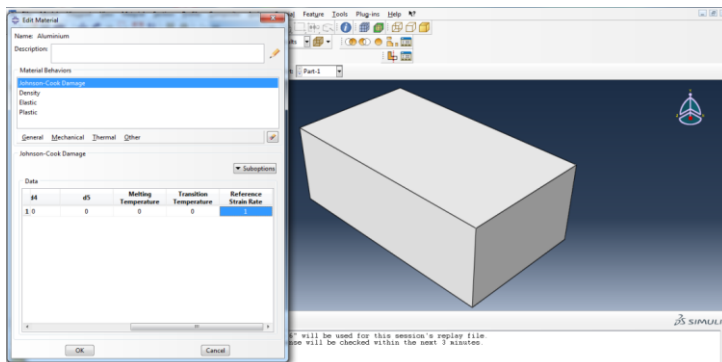


Figure 3.29: Reference strain rate of Aluminium

21. Click the “Sub-option” to apply Damage Evolution, the displacement at failure is 0.0001.

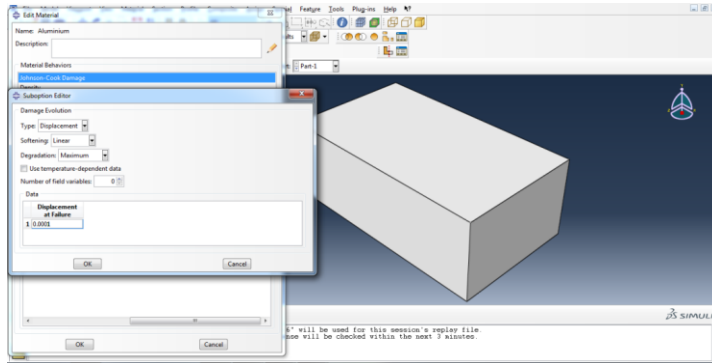


Figure 3.30: Damage evolution of Aluminium

22. Apply the material properties of High Speed Steel.

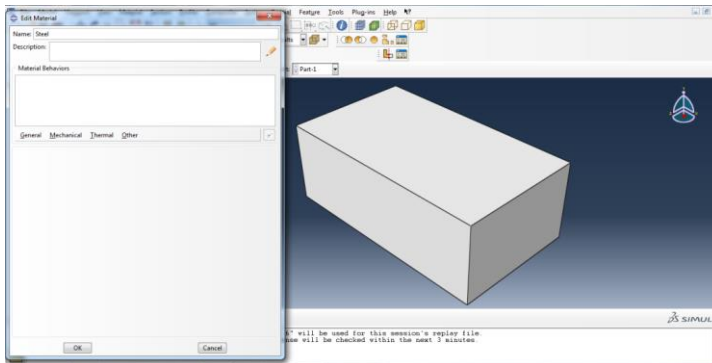


Figure 3.31: Material properties of high speed steel

23. Fill in the value of density of steel, the density of high speed steel is 7870 kg/m^3 .

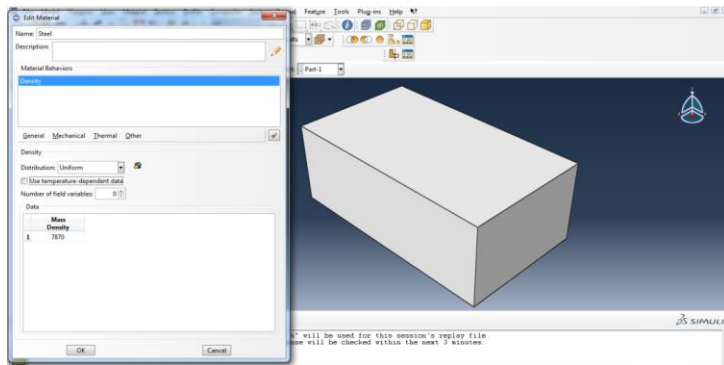


Figure 3.32: Density of high speed steel

24. Fill in the value of Young's Modulus and Poisson Ratio. The young modulus of is 200 GPa and Poisson's ratio is 0.29.

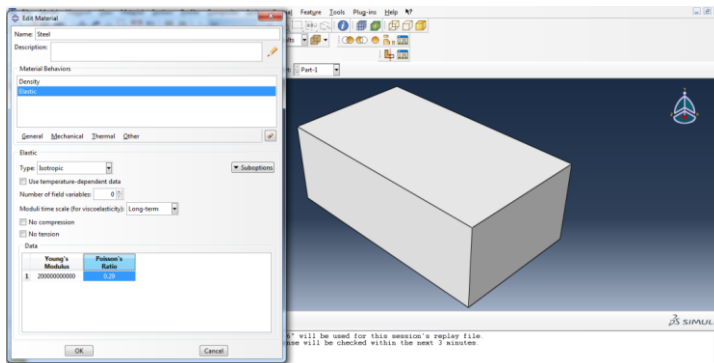


Figure 3.33: Elastic properties of high speed steel

25. Fill in the Plastic Properties by using Johnson Cook Model.

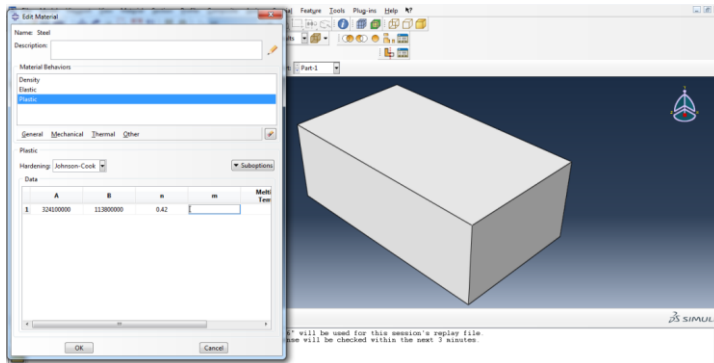


Figure 3.34: Johnson Cook material properties

26. Fill in the value of Johnson Cook Damage Failure Model.

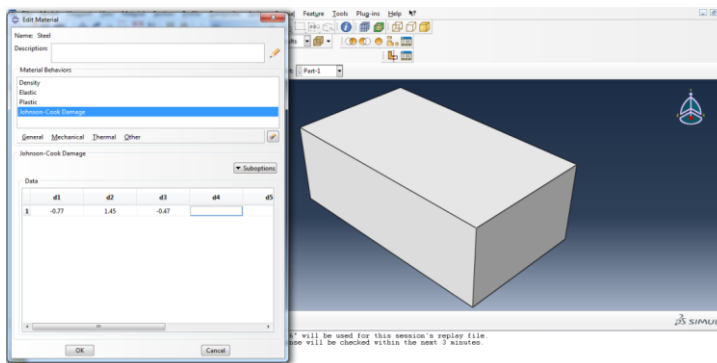


Figure 3.35: Johnson Cook material properties

27. Fill in the value of Reference Strain Rate.

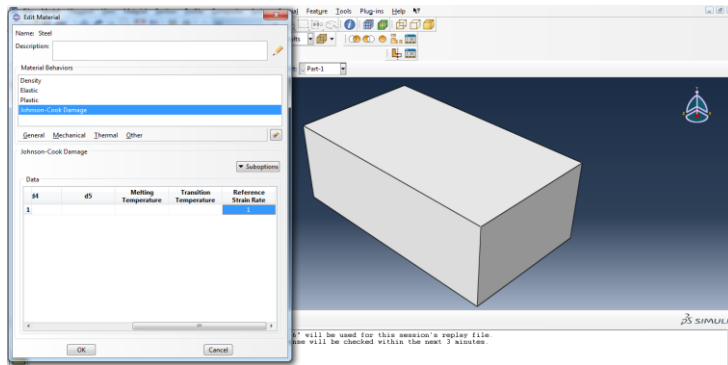


Figure 3.36: Reference strain rate

28. Click the “Sub-option” to apply Damage Evolution.

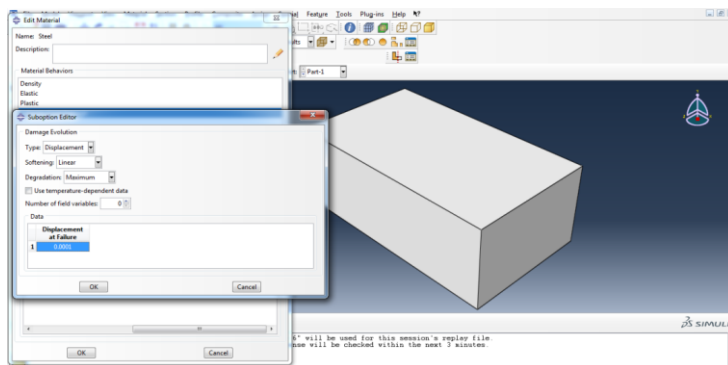


Figure 3.37: Damage evolution

29. Create the Section for both of the materials, first is Aluminium.

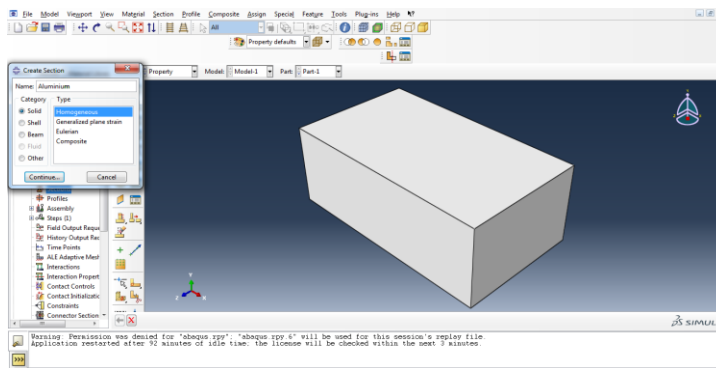


Figure 3.38: Aluminium section

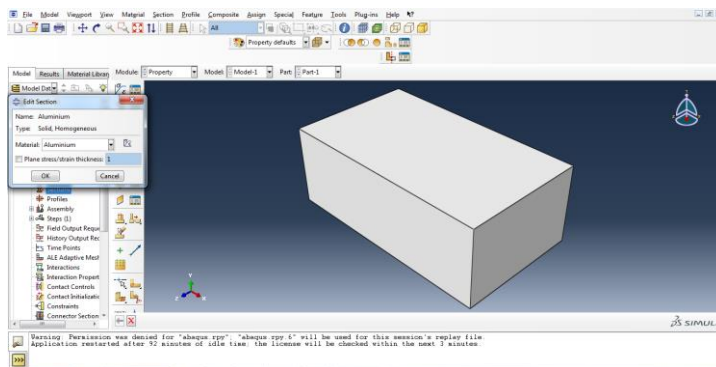


Figure 3.39: Aluminium section

30. Second is Steel.

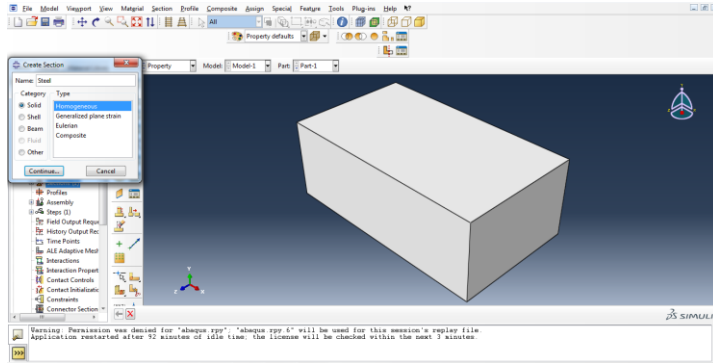


Figure 3.40: Steel section

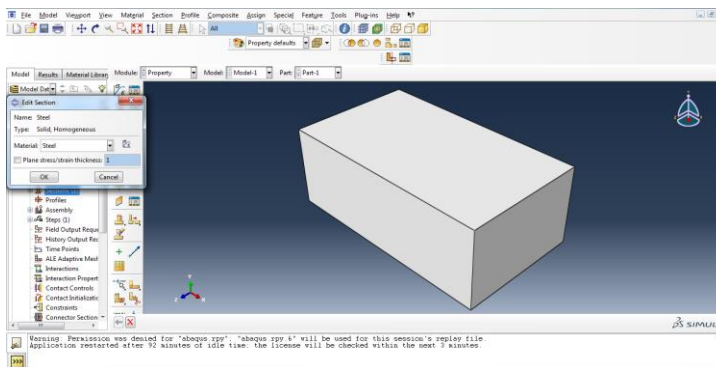


Figure 3.41: Steel section

31. Create the partition at the top of the raw material to specify the part to be removed during side milling.

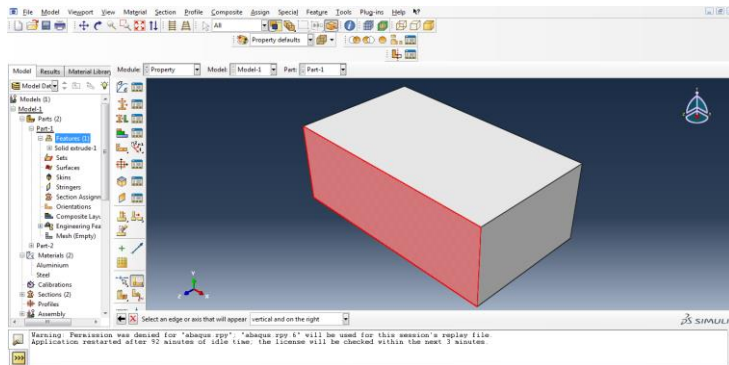


Figure 3.42: Create partition

32. Draw a line which the distance from the top of raw material is 0.004.

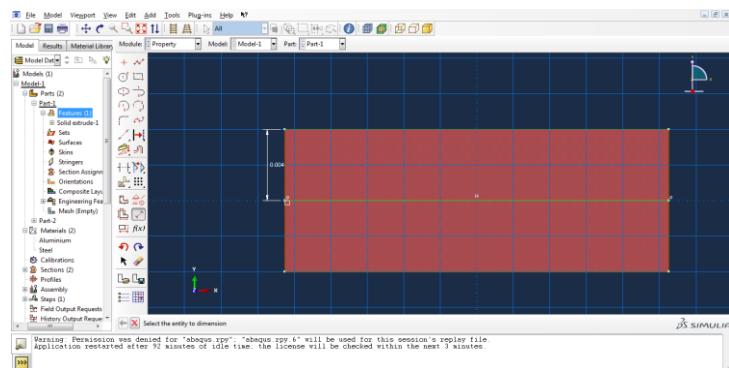


Figure 3.43: Line of partition

33. Use the “Partition Cell” Function to create partition.

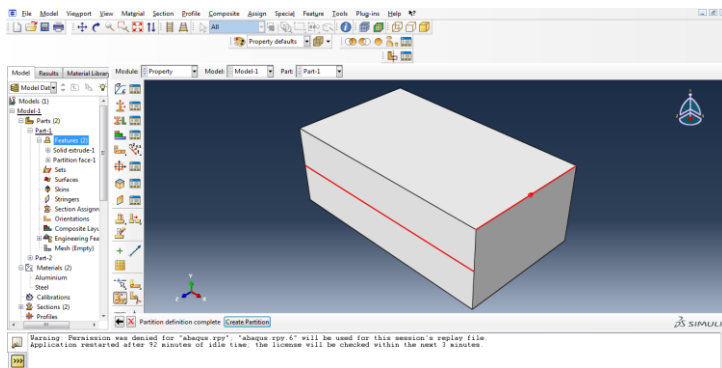


Figure 3.44: Partition cell

34. Define the lower and upper part of raw material to become Aluminium.

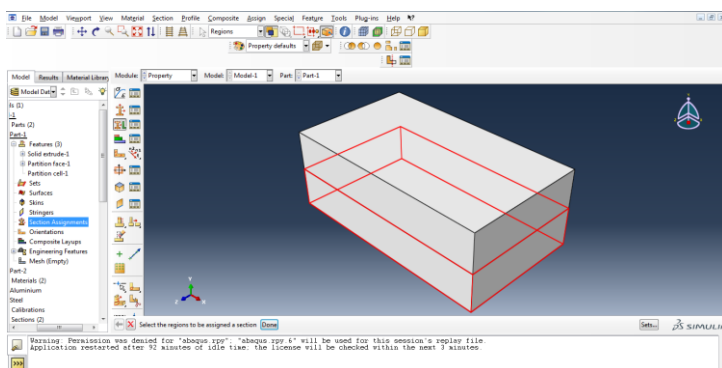


Figure 3.45: Define it become Aluminium

35. Choose “Aluminium” for lower and upper part.

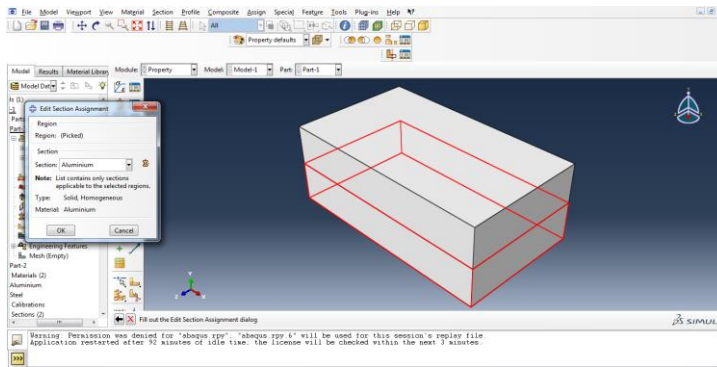


Figure 3.46: Define both part become Aluminium

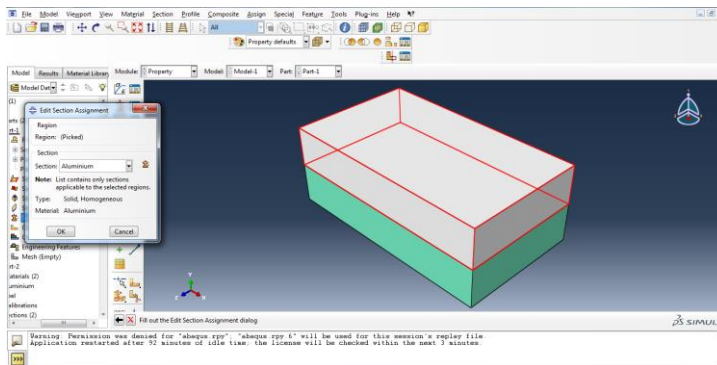


Figure 3.47: Define both part become Aluminium

36. Define the material of cutting tool to become “Steel”.

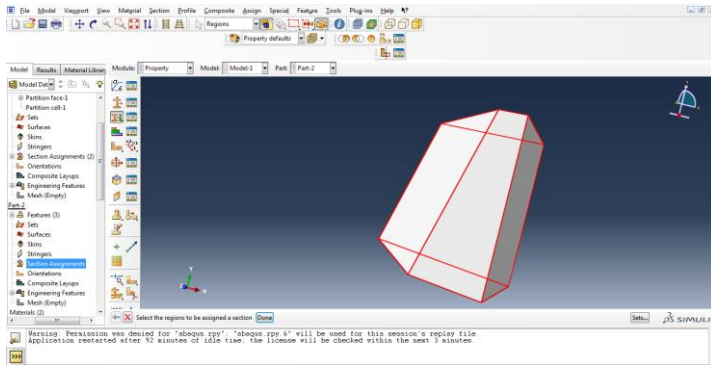


Figure 3.48: Define steel material

37. Put the instance into same workbench by using assembly function.

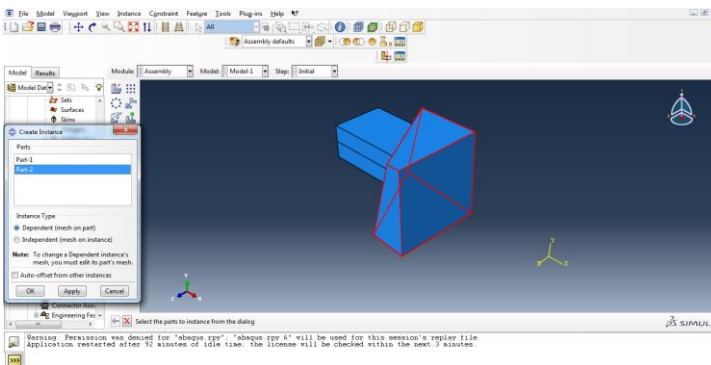


Figure 3.49: Assembly workbench

38. Use the “Translate” and “Rotate” function to adjust the position of the cutting tool and raw material. Thus, the position of the cutting tool will move in Y direction and the part to be milled is tangential to the cutting tool.

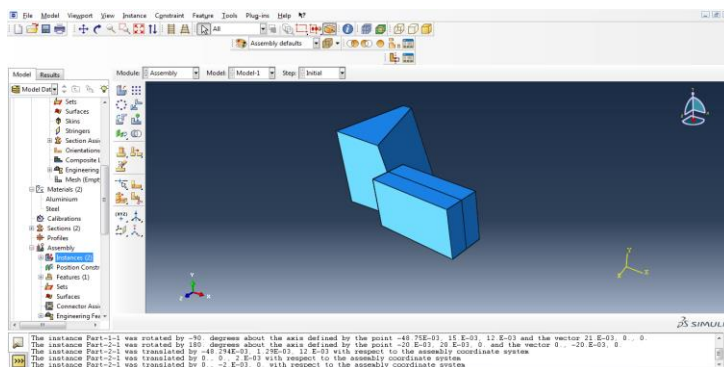


Figure 3.50: Position the cutting tool and workpiece

39. Create the Step which is “Dynamic, Explicit”. Since the simulation is metal cutting which is dynamic movement.

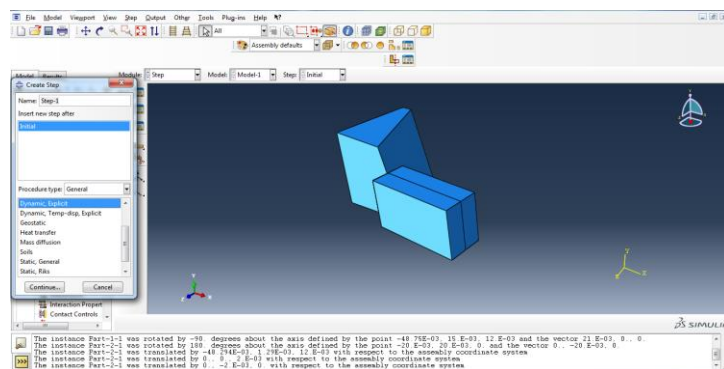


Figure 3.51: Create step

40. Next, set the time period of the step become 0.504 second.

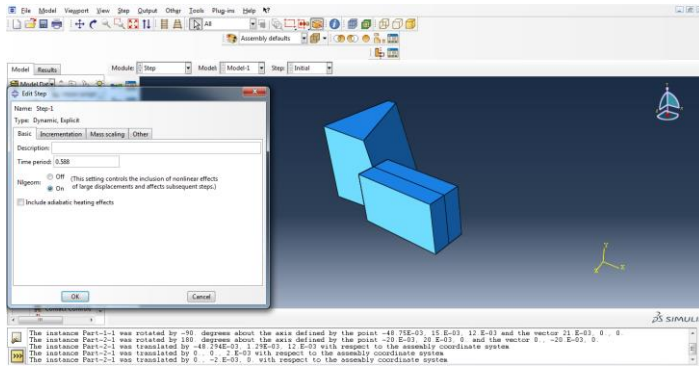


Figure 3.52: Time period

41. Define the interaction properties between the cutting tool and raw material, the type of contact between two parts is “contact”.

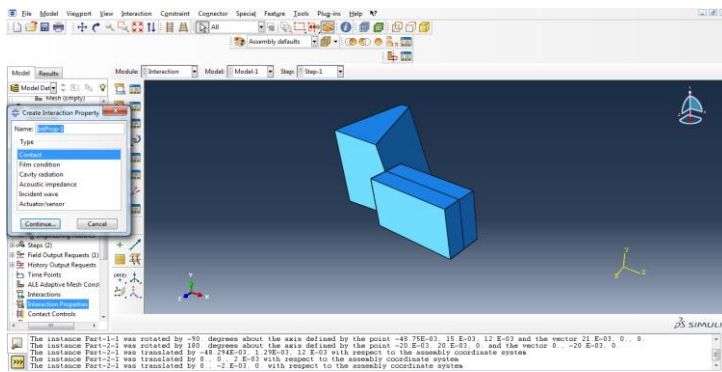


Figure 3.53: Interaction properties

42. Choose the mechanical part, and then “Tangential Behavior”, the friction formulation in this simulation is “Penalty”. Lastly, the friction coefficient is 0.15.

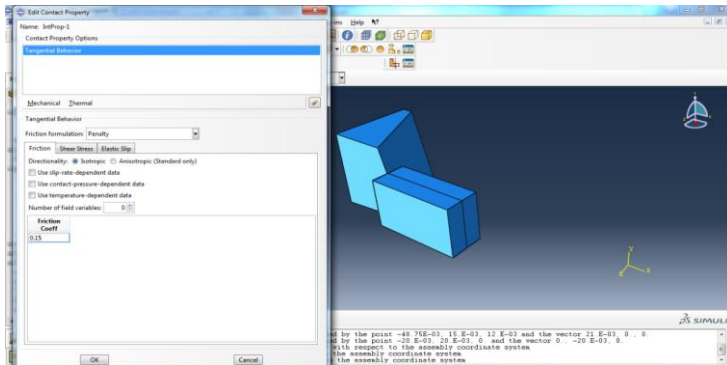


Figure 3.54: Friction coefficient between two materials

43. To the interaction, select the “General Contact (Explicit)”.

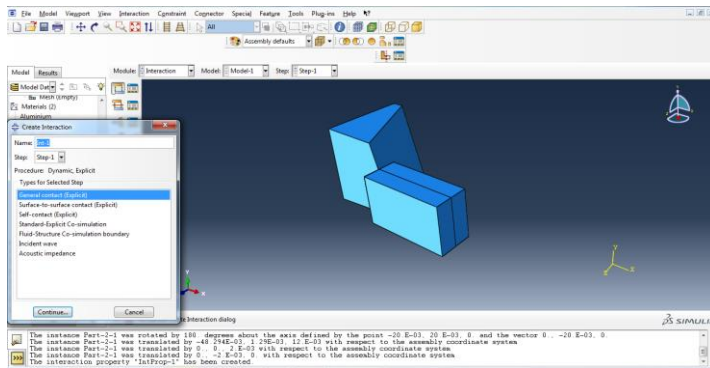


Figure 3.55: Interaction general contact

44. In the Attribute Assignment, the global property assignment is set as before, which is “IntProp-1”.

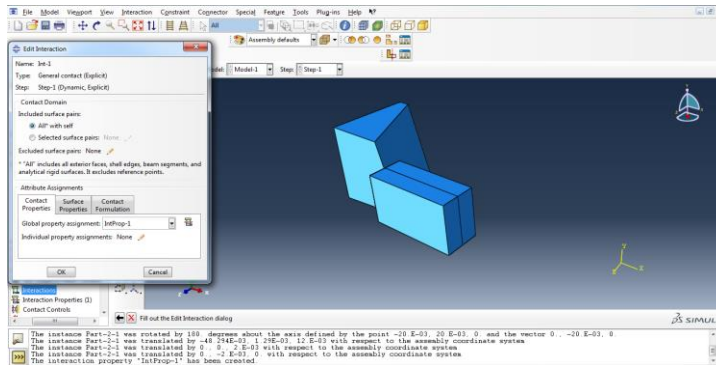


Figure 3.56: Attribute assignment

45. Create the surface which will make contact to the raw material, there are two surface from the cutting tool.

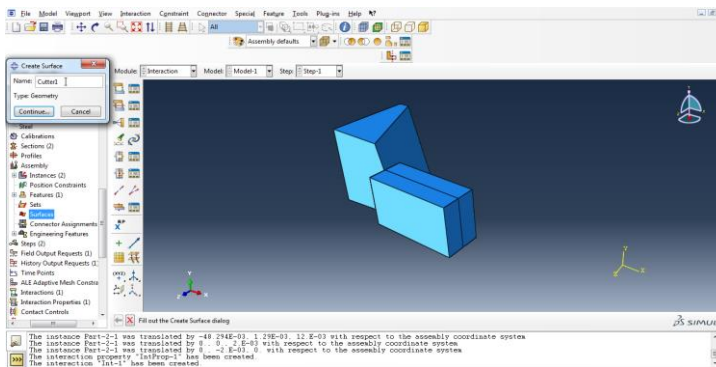


Figure 3.57: Create surface

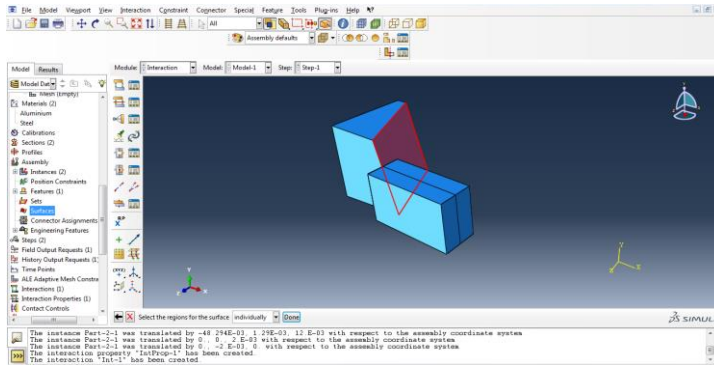


Figure 3.58: Create rake surface

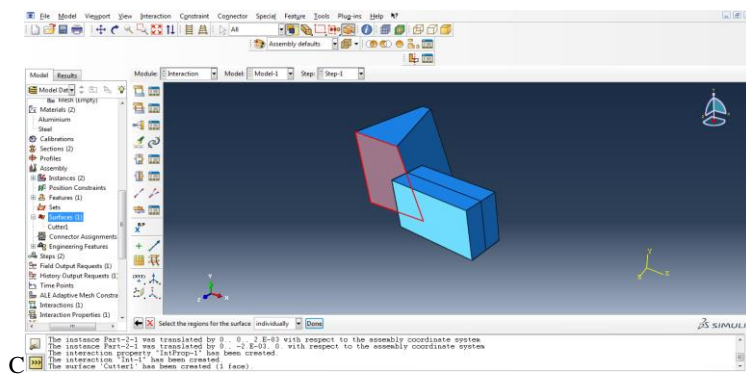


Figure 3.59: Create clearance surface

46. Create and set the boundary condition of raw material.

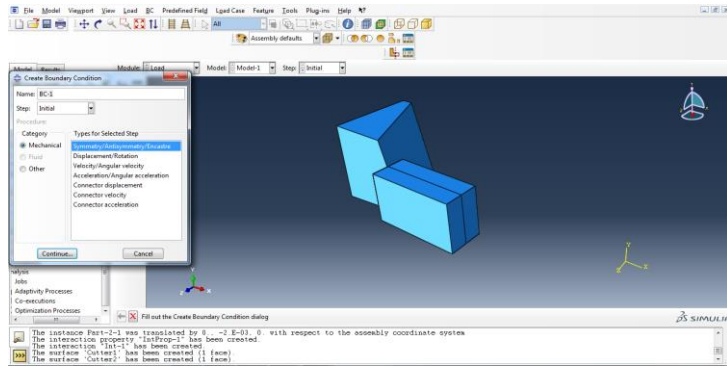


Figure 3.60: Create boundary condition

47. Bottom of the raw material has been selected because it remain stationary.
ENCASTRE ($U_1=U_2=U_3=UR_1=UR_2=UR_3=0$).

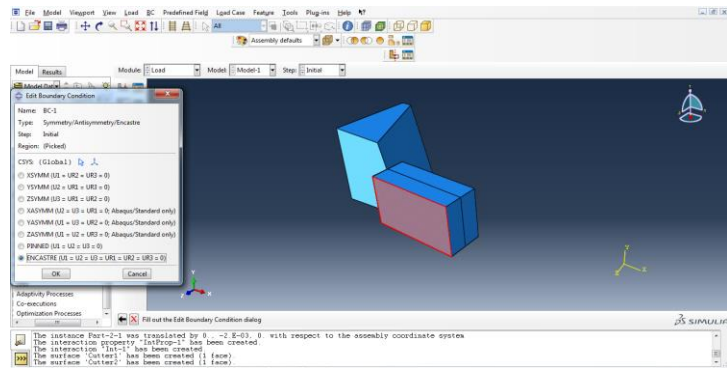


Figure 3.61: Fix the bottom surface of workpiece

48. Create and set the boundary condition of cutting tool. The choice is “Displacement/Rotation”.

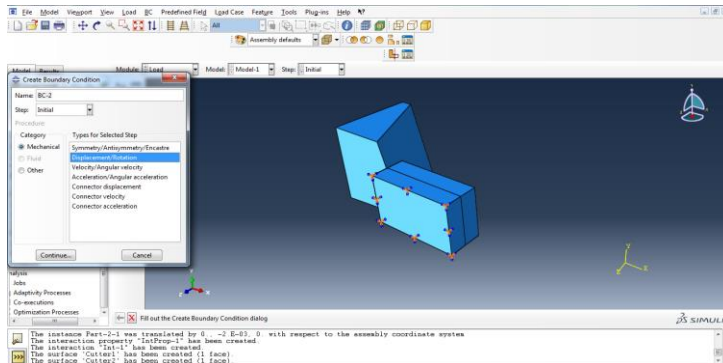


Figure 3.62: Cutting tool boundary condition

49. After selected the cutting tool, tick all of the direction which are U1, U2, U3, UR1, UR2 and UR3.

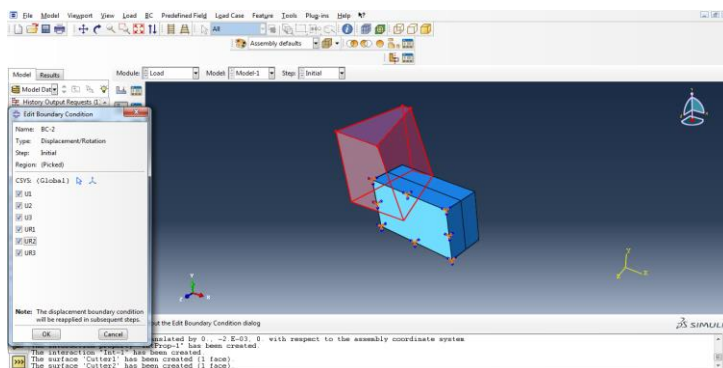


Figure 3.63: Direction available of cutting tool

50. Fill in the value in U2 because it is in Y direction, which is in negative Y-axis with moving 0.024m.

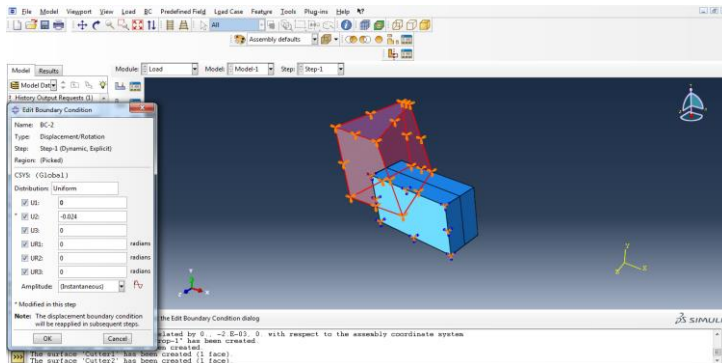


Figure 3.64: Distance of cutting tool moving

51. Fill in the value of time/frequency and amplitude.

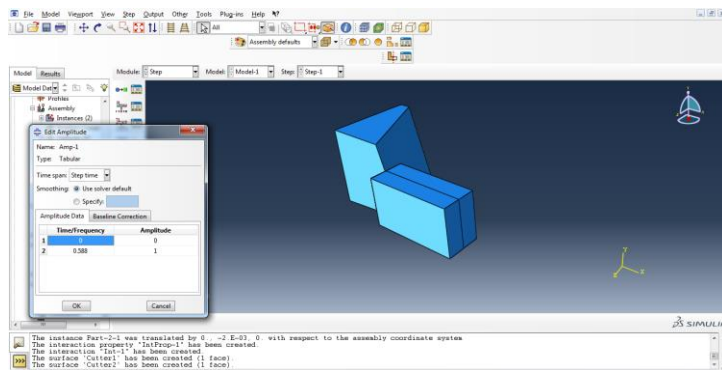


Figure 3.65: Time and amplitude

52. Step to mesh the raw material, decide the global seed of the part.

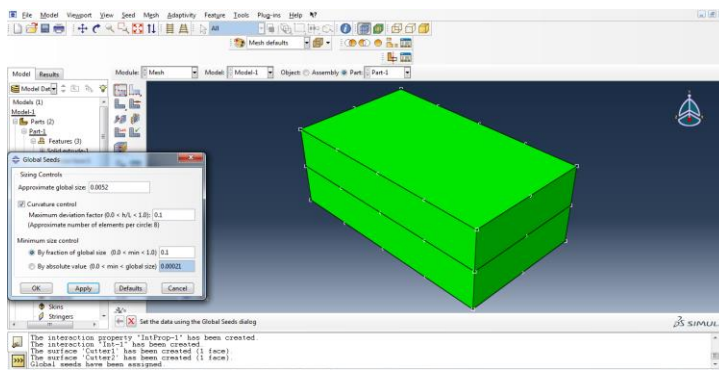


Figure 3.66: Global seed of the part

53. Change the view to “wireframe” so that meshing will be easily. Choose the edge to apply local seeds. Apply 20 elements for the vertical edge of upper part.

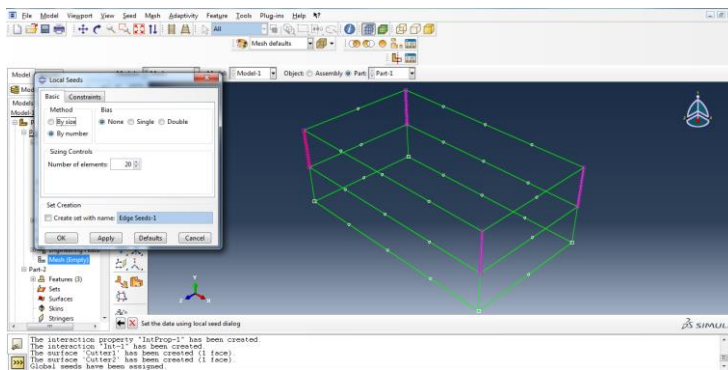


Figure 3.67: Edge local seed by using numbering method

54. Apply 200 elements for the horizontal edge of upper part.

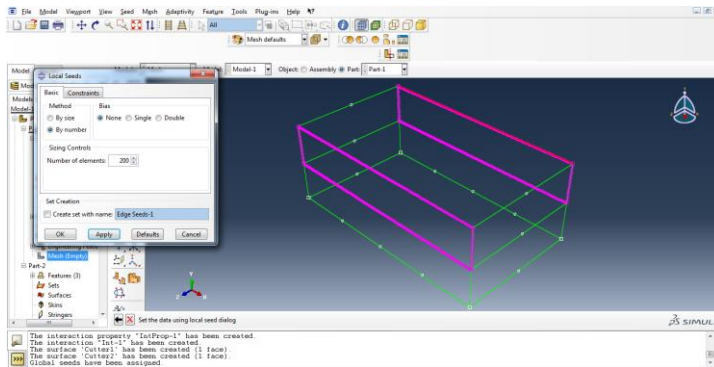


Figure 3.68: Number of element for horizontal edge

55. Mesh and control the lower part of raw material by using “sweeping” technique.

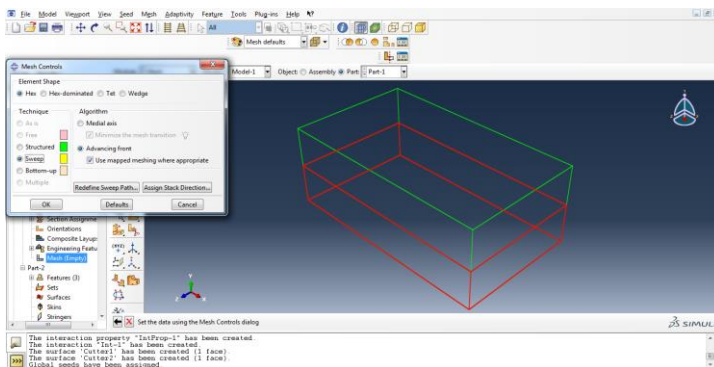


Figure 3.69: Mesh and control the lower part

56. For the upper part of raw material, it use explicit element type and it has been set to element deletion.

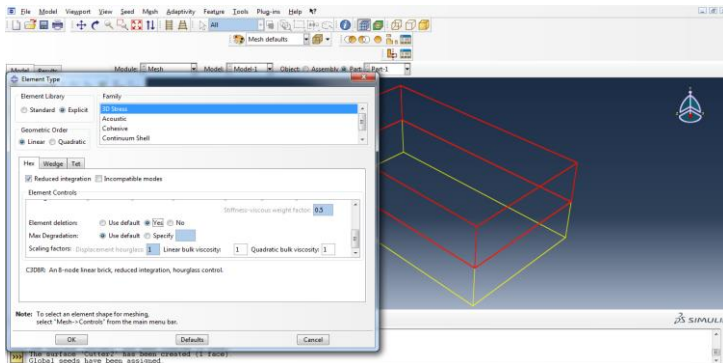


Figure 3.70: Explicit element type for element deletion

57. Mesh the part.

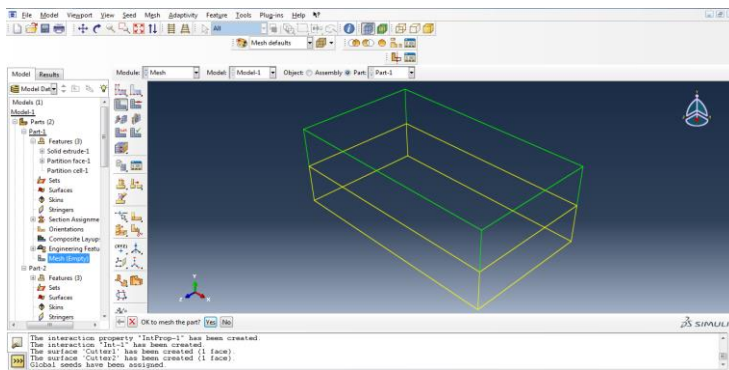


Figure 3.71: Mesh the part

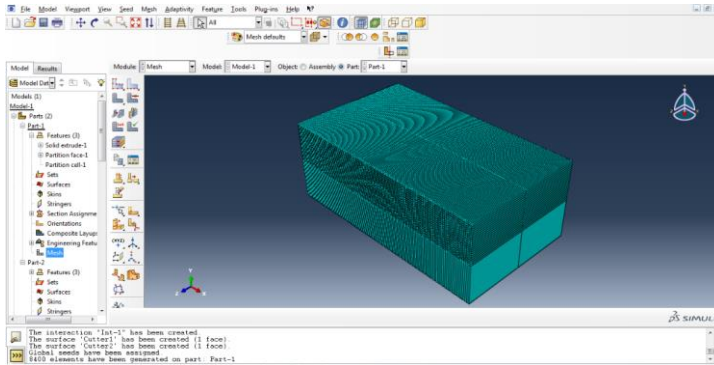


Figure 3.72: After meshing

58. Mesh the cutting tool by applying the global size to 0.0023.

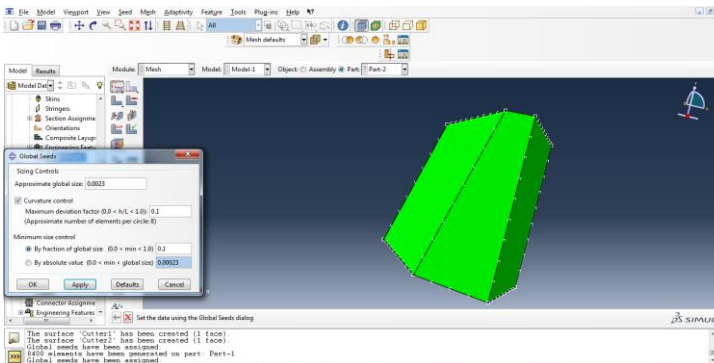
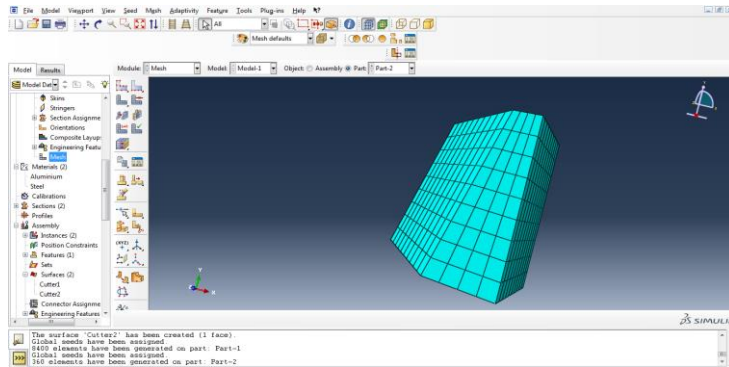
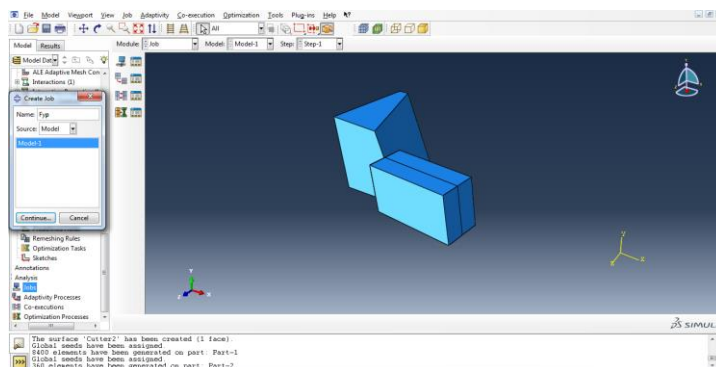


Figure 3.73: Global size of cutting tool

59. Mesh the part.**Figure 3.74: Mesh the part****60. Create the job.****Figure 3.75: Create the job**

61. Edit the field output request. Select the STATUS which include the some failures and plasticity model.

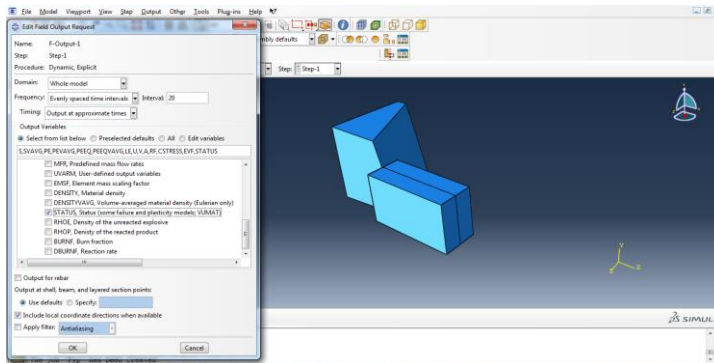


Figure 3.76: Status output for some failure and plasticity model

62. Submit the job until the step time increment reach 0.588 second.

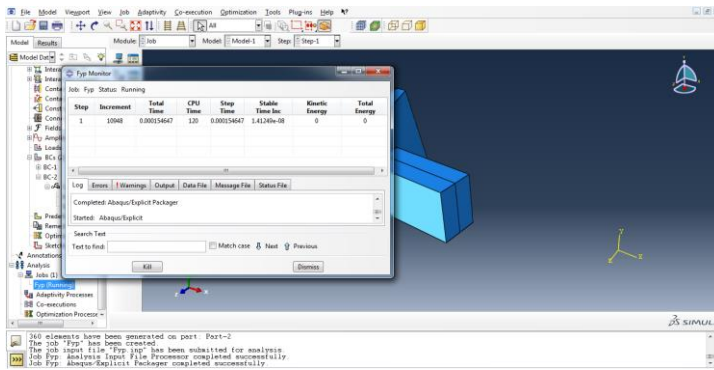


Figure 3.77: Job submission

3.8 DESIGN OF EXPERIMENT

First of all, part of aluminum has been cut from a long aluminium using the horizontal band saw machine. The aluminium was in the dimensions of 10.6 cm x 10.4cm x 15cm. Next, the aluminium workpiece has cut using wire EDM cut machine to reduce the thickness of the workpiece material. The thickness has reduced to 2cm. The thickness has to be reduced to suit the dimensions of the dynamometer. Figure 3.78 shows the EDM Wire Cut machine is cutting the workpiece material into two pieces.



Figure 3.78: Cutting workpiece material using wire cut

Next, the workpiece material was taken from the machine and proceeded to the milling machine to remove the surface that is not even. The workpiece material will reduced in thickness until 1.2cm. Figures 3.79 shows the workpiece material after face milling process.

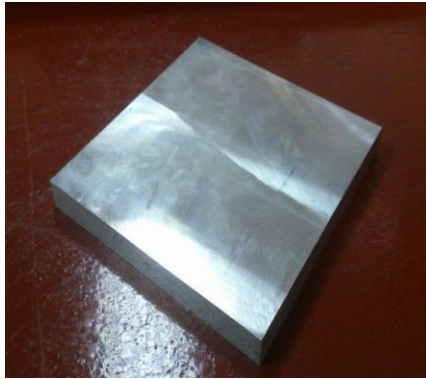


Figure 3.79: Complete Workpiece Material

The equipment and tools used in this experiment was Haas VF-6 milling machine. First of all, Kistler dynamometer was clamp on the working platform of milling. The workpiece material was then clamped on the top of dynamometer. Figure 3.80 shows the workpiece material was clamped and prepared to conduct the experiment.



Figure 3.80: Workpiece material on dynamometer

The dynamometer was then connected to the amplifier to make sure all the data will be converted and sent it to data acquisition software, Dyno-ware. Meanwhile, the

Dial Test Indicator is used to ensure the vice fixed jaw is in the relation of the centerline of spindle. Figure 3.81 shows the DTI was adjusting before experiment.



Figure 3.81: Dial Test Indicator.

The experiment setup was shown in Figure 3.82. The dynamometer is clamp on the milling table and it is connected to the amplifier. Lastly, the amplifier is connected to the laptop with the Dyno-ware software.



Figure 3.82: Experiment Setup

The experiment start with side milling process which cut the right hand side of the workpiece material using 12mm end mill as shown in figure 3.83. The experiment was started from spindle speed with 4851 RPM. However, the appropriate feed per tooth used in this experiment is 0.005 inches per tooth, the feed rate was calculated which is 48.51 inches per minute. The depth of cut is 2mm in X direction since it is side milling process. The estimated cutting time is 3second. Thus, all the important parameters was set before the experiment. The cutting process has started simultaneously with the data acquisition system to get the accurate results from dynamometer. Figure 3.84 shows that after one cutting through 2mm, the machining was stopped to obtain the chip formation and cutting force.



Figure 3.83: 12 mm End Mill

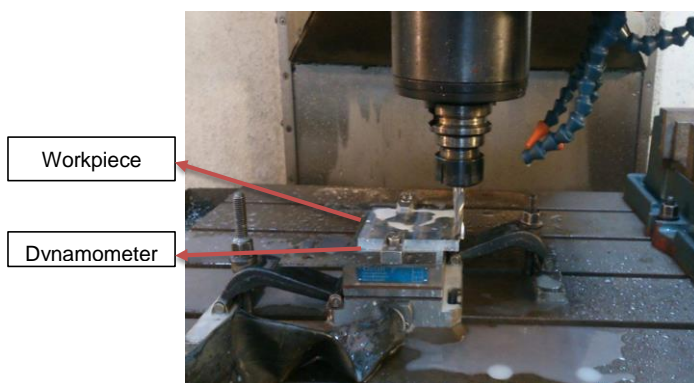


Figure 3.84: After the experiment

CHAPTER 4

RESULT AND DISCUSSION

4.1 INTRODUCTION

This chapter covers and discusses about the results obtained from the experiment and simulation through dynamometer and ABAQUS respectively. Discussion also had been made in order to have better understanding for the results in detailed manner.

4.2 RESULTS

4.2.1 Effects of Machining Parameters ~~to~~ on the Cutting-cutting Forces

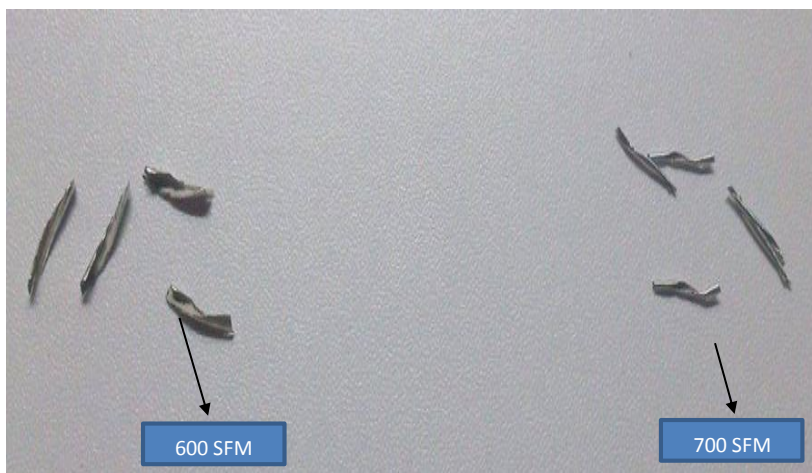


Figure 4.1: The Chip Formation of Experiment

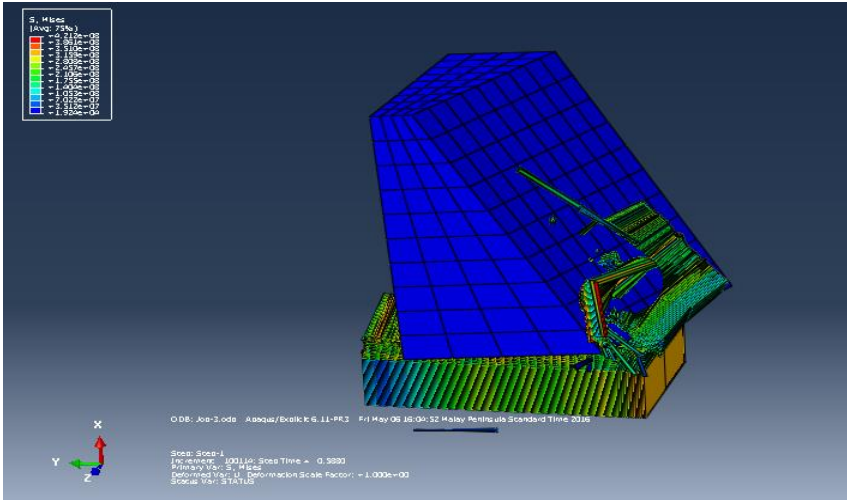


Figure 4.2: 600 SFM Metal Cutting Simulation

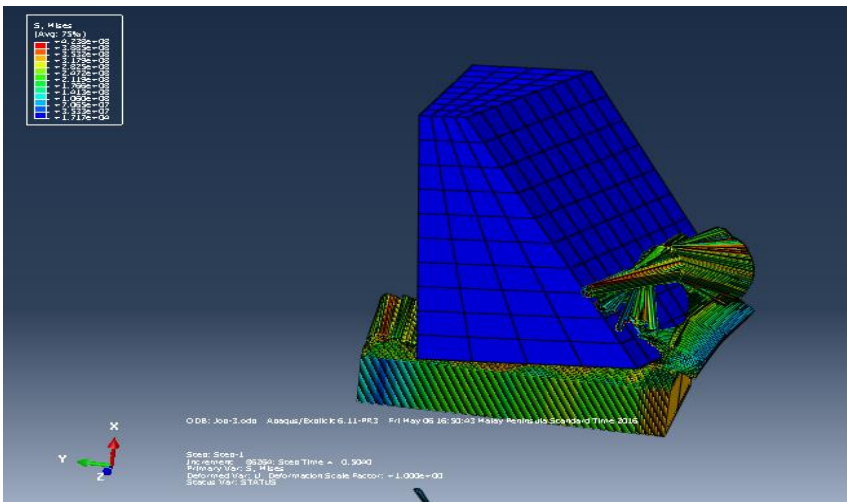


Figure 4.3: 700 SFM Metal Cutting Simulation

It is observed that the cutting force was increased when the cutting speed increased. In fact, the cutting force was supposed to **increase** only when the cutting force ~~is~~ decreased. This will happen due to the ~~factor of~~ thermal reaction which we call thermal softening which changes the shear angle and thus also the plastic deformation. Thus, it can be concluded that the cutting process causes the shear conditions appear and thus the forces required decreased (Subramanian et al. 2013). However, the increasing cutting speed which led to reduction of cutting force is due to the friction force between the cutting tool and workpiece. Thus, this situation is in the agreement with the existed findings which says that the cutting force decreased when the cutting speed increased (Şeker et al. 2004). But however, the scenario which stated above in when the feed rate was held constant, the parameters used in this project was 600 SFM and 700 SFM only and the feed rate was 4851 RPM and 5660 RPM respectively. Thus, the theoretical cutting time of both cutting speed also different.

Next, the chip formation observed in the both 600 SFM and 700 SFM cutting speed shows the difference in size and thickness. Figure 4.1 clearly shows that the chip formation obtained after the side milling process. The chips formation from experiment shows that the thickness of chips from 600 SFM is bigger than chips from 700 SFM. This is due to the velocity flow of cutting the raw material is high in 700 SFM, and this will affect the thickness of chips which produced the small thickness chips compare to 600 SFM. Nevertheless, the chips observed between experiment and simulation shows similarities. Figures 4.2 and 4.3 shows the side milling process with 600 SFM and 700 SFM respectively. It can be observed that the chip formation from simulation have shown the C-type with upwards curling. Moreover, the size and thickness of chip formation from simulation displayed difference. 700 SFM shows smaller and thinner chip formation if compare with 600 SFM. However, the chips formation of both cutting speed shows that they are continuous chips. Moreover, the chip form classification belongs to C-type with upwards curling, then the level of curl for both chips formation was completely different. It can be observed that the higher the cutting speed will have curlier chips.

Commented [U1]:

4.2.2 Cutting Force between Experimental and Theoretical Results

Figures 4.4 and 4.5 show the radial force generated during the 600 SFM and 700 SFM. The average force of 700 SFM shows higher value than 600 SFM because the feed rate parameters changed. From the Figure 4.4 and 4.5, the highest force for 600 SFM shows approximately 168 N whereas the highest force for 700 SFM shows approximately 180 N. The feed rate affects the force produced because when the velocity of the spindle increased along the direction of cut, the material removed with faster velocity too, thus the force required will be higher. However, the highest force required between 600 SFM and 700 SFM has no much difference because the cutting speed was high enough to remove the materials.

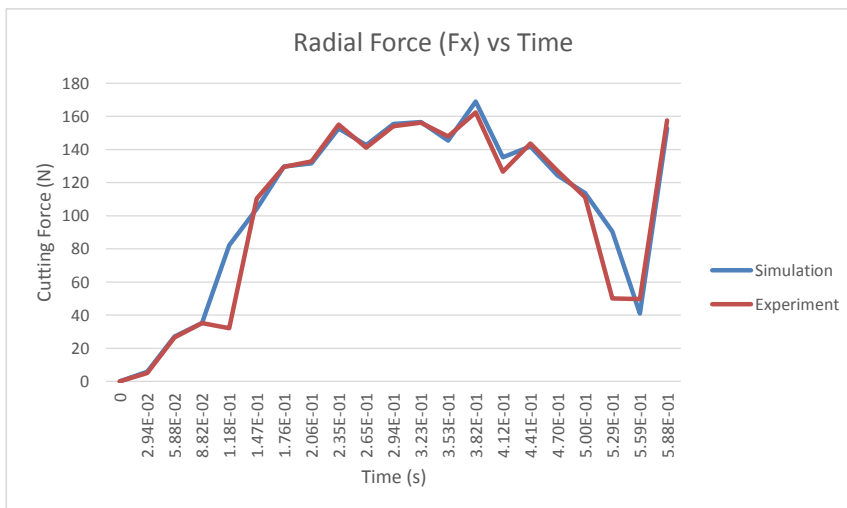


Figure 4.4: 600 SFM Radial Force

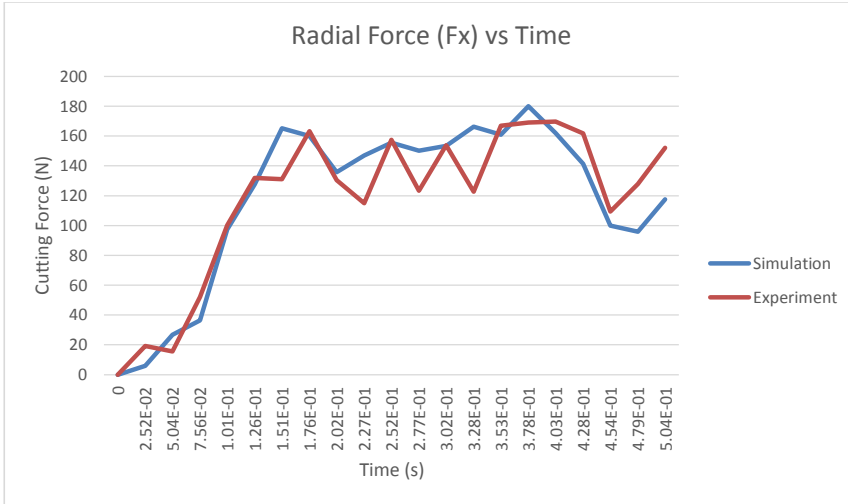


Figure 4.5: 700 SFM Radial Force

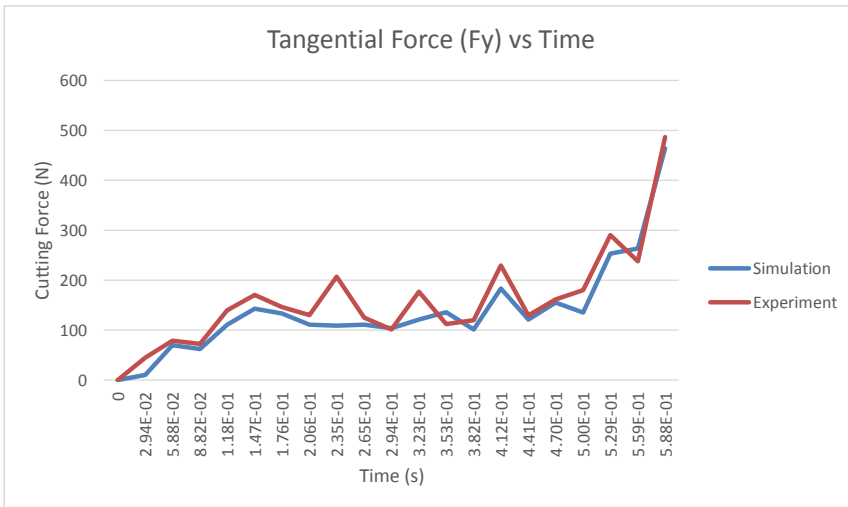


Figure 4.6: 600 SFM Tangential Force

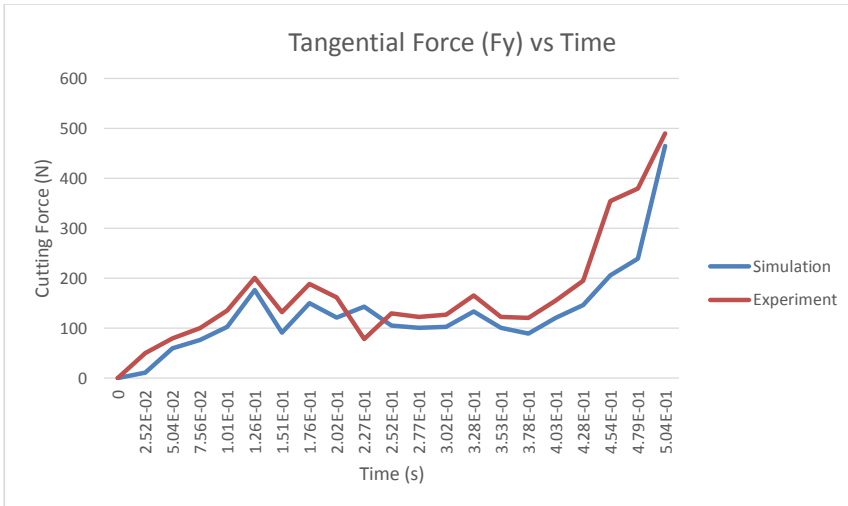


Figure 4.7: 700 SFM Tangential Force

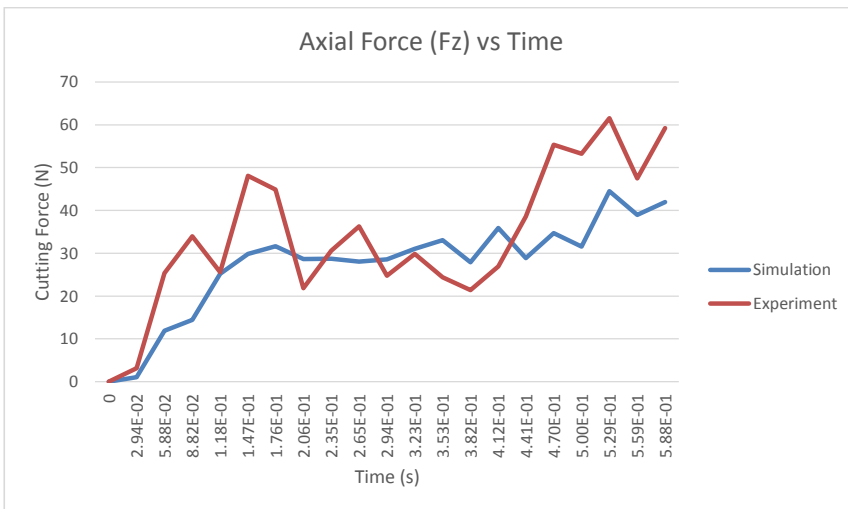


Figure 4.8: 600 SFM Axial Force

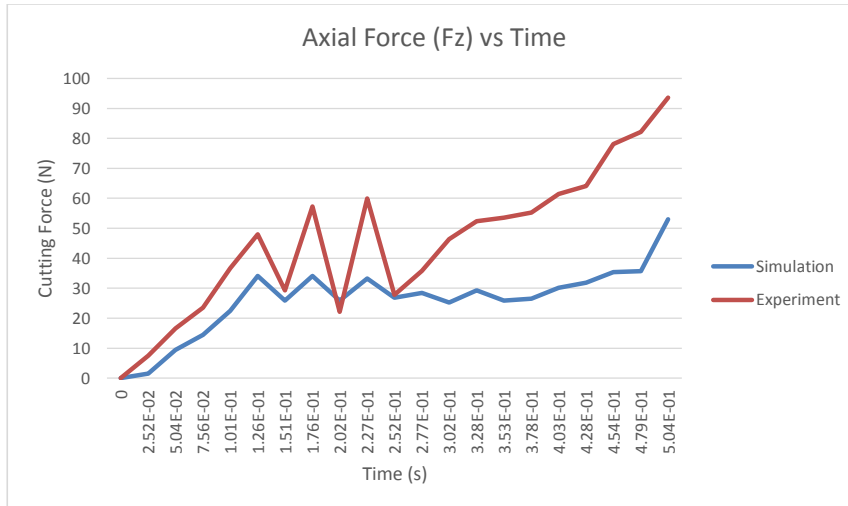


Figure 4.9: 700 SFM Axial Force

~~Figures 4.4 and 4.5 show the radial force generated during the 600 SFM and 700 SFM. The average force of 700 SFM shows higher value than 600 SFM because the feed rate parameters changed. From the Figure 4.4 and 4.5, the highest force for 600 SFM shows approximately 168 N whereas the highest force for 700 SFM shows approximately 180 N. The feed rate affects the force produced because when the velocity of the spindle increased along the direction of cut, the material removed with faster velocity too, thus the force required will be higher. However, the highest force required between 600 SFM and 700 SFM has no much difference because the cutting speed was high enough to remove the materials.~~

Figure 4.5 and 4.6 shows the tangential force generated during the 600 SFM and 700 SFM. It is obvious that tangential force was shows the highest cutting force among the three direction of force. This force is acting in the direction of the cutting tool in which it was cut from inside out in Y-direction. From Figures 4.6 and 4.7, it can be inferred that tangential force was the highest because more flute will be get engaged in the cutting process which has results more cutting force. Furthermore, the area of the

flute has involved in the cutting process in the rotating direction indicates that higher cutting force was required to remove the materials (Subramanian et al. 2013).

Figure 4.8 and 4.9 shows the radial force generated during 600 SFM and 700 SFM. Radial force was acting in the direction of radial axis of cutting tool, which is in the direction of Z-axis when observed in the machining process. However, this force shows the lowest among three direction of force. This happened because the machining process is side milling, thus the cutting tool has cut the right hand side of the material workpiece, which means that there were no resultant force having in the Z-direction. But however, the force obtained in 700 SFM is higher than 600 SFM. This is due to the feed rate increased from 1232.15 cm/min to 1437.51 cm/min results the higher thrust force in Z-direction.

Next, the cutting forces obtained in three direction which are radial, tangential and axial force shows deviation between experimental and theoretical results. However, there are many factors would had affected the results for both experimental and theoretical. But from the Figure 4.4 to 4.9, it can be observed that the cutting forces of 700 SFM with radial, tangential and axial direction shows bigger variance between experiment and theoretical. This is because in this project the chatter and tool wear had not been taken into consideration. The higher cutting speed and feed rate which will results more chatter and vibration causes by high spindle speed and also friction between material workpiece and cutting tool. Other than that, the cutting force measurement in experiment will not be 100% accurate with theoretical due to machine capability and manual calibration. It has been proved and demonstrated that the method of meshing in the simulation which was Eulerian approach (Jeevannavar & Hussain 2014). Eulerian method is the most effective method for detailed studies in chip formation because it implies the shape and size of chip formation, shear zone angle, and also the contact conditions of cutting tools and material workpiece (Markopoulos & Books24x7 Inc. 2013).

4.2.3 Stresses of Cutting Process

Figure 4.10 and 4.11 shows the stress distribution of both 600 SFM and 700 SFM cutting speed. The simulations were conducted successfully as it was observed different zone of material being removed shows different temperature distribution. Figures 4.10 and 4.11 have clearly show that the primary and secondary zones are seen

with the highest stress area. The residual stress in this situation was hard to be determined because the clearance angle of the cutting tool is 5° . Since that the residual stress was generated along the machined surface (Adetoro & Wen n.d.).

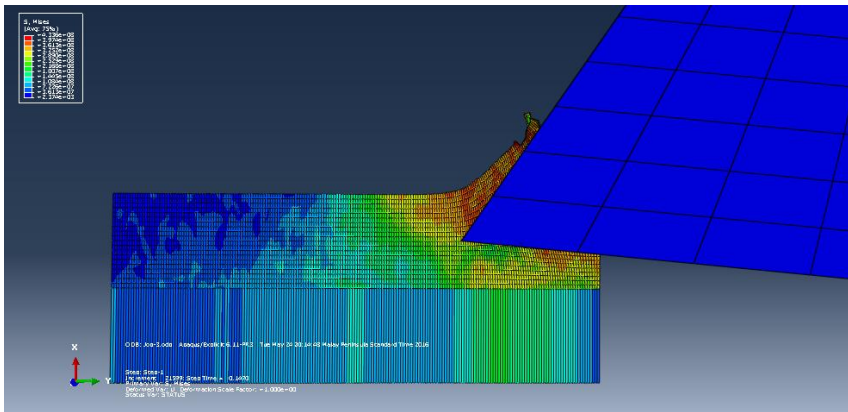


Figure 4.10: Stress Distribution of 600 SFM.

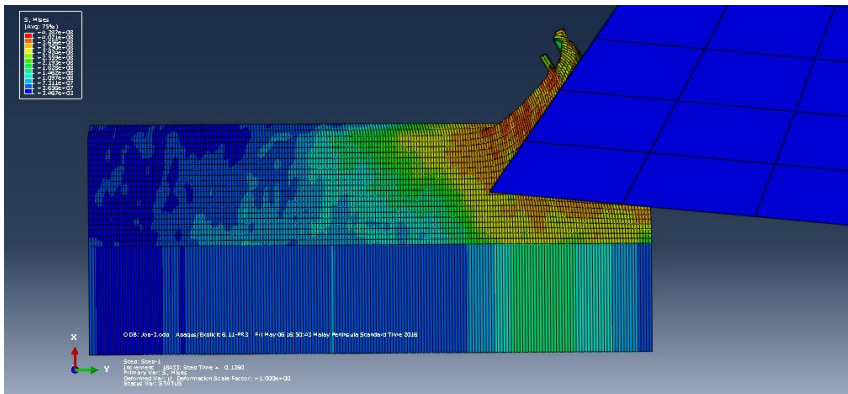


Figure 4.11: Stress Distribution of 700 SFM.

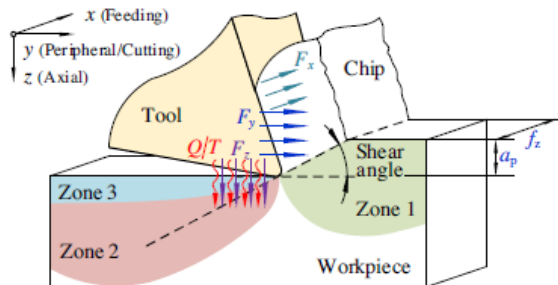
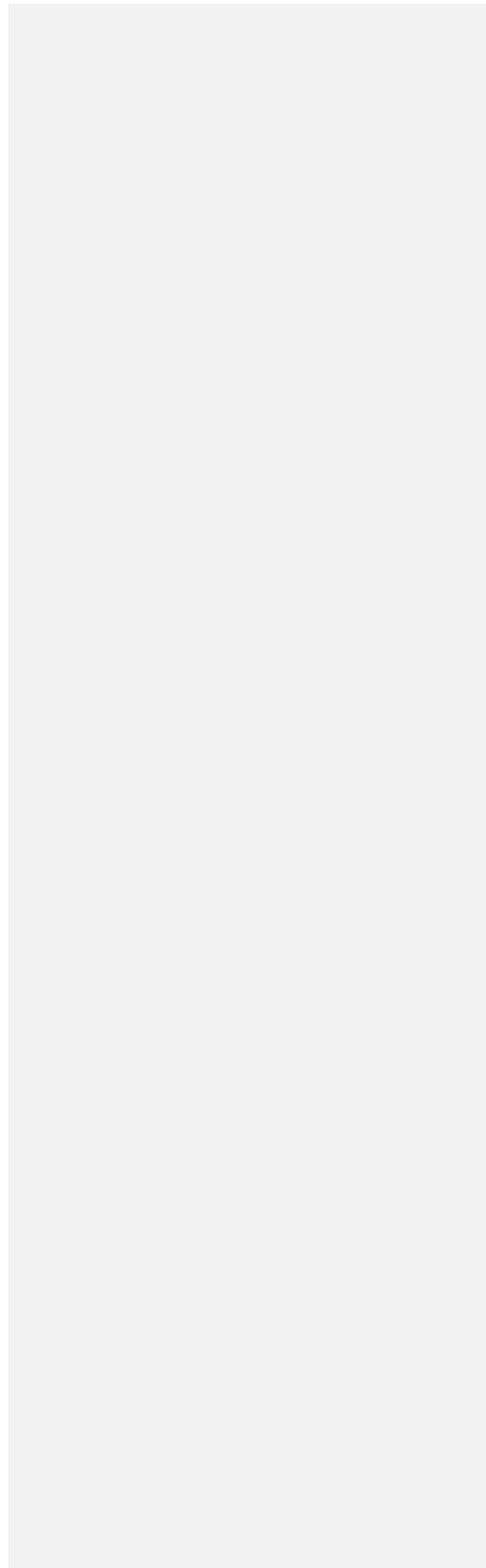


Figure 4.12: Simplified Analytical Model of the Stress Zones(Ma et al. 2016)

Figure 4.12 shows simplified analytical model of the stress zones. This model can explain the machining situation between cutting tool and material. When the cutting tool was cut the material, zone 3 undergoes plastic deformation. Meanwhile, frictional force between reliefs face and machined surface, which is the results of tangential force and radial force in this case. Both of these force were intended to introduce tensile plastic strain in the surface layer and tensile elastic strain in the inner part of the material. Thus, compressive stress in the surface layer has been introduced because of elastic strain has been released. This happened after the machining. Apart of that, there was stress happened in zone 2 in both of the cutting speed. The stress happened mainly was elastic tensile stress, which is caused by the shear movement in the shear deformation zone. After that, same situation happened which is compressive stress has been introduced in the surface layer(Ma et al. 2016).



CHAPTER 5

CONCLUSIONS AND RECOMMENDATIONS

5.1 INTRODUCTION

This chapter summarizes the study by coming up with conclusions which are made based on the results obtained and discussed. ~~This chapter~~It also includes recommendations that could be done for future studies and solution.

5.2 CONCLUSIONS

The purpose of this project ~~is~~was to study the machining parameters that will influences the chip formation of the side milling. The machining parameters was the variables that we can control in order to produce the desired shape of material workpiece. Meanwhile, prediction of cutting force during the machining processes would define weather the machining parameters are in the appropriate and correct scope. Cutting force generated in the machining process has been predicted using the simulation which was ABAQUS. The results and data obtained in both experiment and simulation are similar although some of them were not match. However, the results that we obtained in this project has already achieved the objectives. The machining process performance can be improved by prediction of the cutting force and then the chip formation could be compared to produce ideal finished products.

As a conclusion, the objectives of this project has been achieved. The cutting speed, radial depth of cut, feed rate and etc. will affect the chip formation and thus the finish products. The optimization of milling performance can be improved by setting up the parameters correctly.

5.3 RECOMMENDATIONS

This study might have some flaws at certain data or point of opinion where it can be improved for the future studies. A few recommendations has been made which is helpful in order to obtain more precise results and optimization can be done. The following are the recommendations that can be considered.

5.3.1 Cutting Force Measurement Experiment

The cutting force measurement from dynamometer when the experiment was conducted has been affected by many factors such as the timing when started to measure the cutting force in Dyno-ware and the experiment was started to conduct. Because if the timing between both of the step was not accurate, the results precision will be decreased. This can be solved with take several precautions to prevent the imprecise results. One of the steps is try to do both step simultaneously as possible. Other than that, the chatter caused by vibration between cutting tool and material workpiece will also produce the inaccurate result. This can be solved by conducting the experiment several times.

5.3.2 Simulation of Side Milling Process

The simulation model has been done using finite element analysis software which is ABAQUS. The simulation were successfully demonstrated the perfect boundary condition and the ideal cutting force and stress during machining process. Nevertheless, there some limitations which will affect the results of cutting force and stress measurement. One of the limitation is the simulation unable to take consideration of ambient factors such as room temperature. Other than that, the computational time to complete the simulation can increase the cost and time in the industry. However, this can be solved by using the mass scaling method in ABAQUS to reduce the simulation run time without influencing the results.

References

~~This thesis is prepared based on the following references:~~

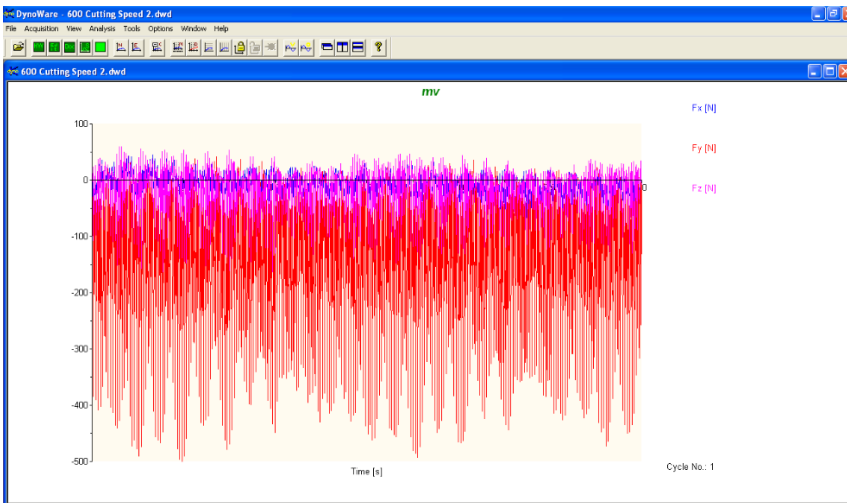
- Adetoro, M.B. & Wen, P.H., Simulation of End Milling on FEM using ALE Formulation . , pp.1–19. Available at: <http://www.simulia.com/forms/world/pdf2008/Adetoro1-AUC2008.pdf>.
- Constantin, C. et al., 3D FEM Analysis of Cutting Processes and simulation and processes. *Simulation*, pp.41–46.
- Group, K., 2009. Multicomponent Dynamometer Type 9257B. , pp.1–4. Available at: www.kistler.com.
- Jeevannavar, A. & Hussain, R., 2014. Process Modelling, Simulation and Experimental Validation for Prediction of Chip Morphology during High Speed Machining of Al 2024-T3. *SAS TECH Journal*, 2014, 13(1), pp.80–87. Available at: http://www.msruas.ac.in/pdf_files/sastechJournals/April2014/11.pdf.
- Ma, Y. et al., 2016. Journal of Materials Processing Technology Prediction of surface residual stress after end milling based on cutting force and temperature. *Journal of Materials Processing Tech.*, 235, pp.41–48. Available at: <http://dx.doi.org/10.1016/j.jmatprotec.2016.04.002>.
- Margot, R. et al., 2005. Monitoring Chip Formation in Machining through Strategical On-line Signal Processing of Acoustic Emission.
- Markopoulos, A.P. & Books24x7 Inc., 2013. *Finite element method in machining processes*,
- Ning, Y., Rahman, M. & Wong, Y.S., 2001. Investigation of chip formation in high speed end milling. *Journal of Materials Processing Technology*, 113(1-3), pp.360–367. Available at: <http://linkinghub.elsevier.com/retrieve/pii/S0924013601006288>.
- Schermann, T. et al., 2006. Aspects of the Simulation of a Cutting Process with ABAQUS/Explicit Including the Interaction between the Cutting Process and the Dynamic Behavior of the Machine Tool. *9th CIRP International Workshop on Modeling of Machining Operations, Bled, Slovenia*, 11, p.12. Available at: <http://scholar.google.com/scholar?hl=en&btnG=Search&q=intitle:Aspects+of+the+Simulation+of+a+Cutting+Process+with+ABAQUS/Explicit+Including+the+Interaction+between+the+Cutting+Process+and+the+Dynamic+Behavior+of+the+Machine+Tool#0>.
- Şeker, U., Kurt, A. & Çiftçi, I., 2004. The effect of feed rate on the cutting forces when machining with linear motion. *Journal of Materials Processing Technology*, 146(3), pp.403–407.
- Subramanian, M. et al., 2013. Optimization of cutting parameters for cutting force in shoulder milling of Al7075-T6 using response surface methodology and genetic algorithm. *Procedia Engineering*, 64, pp.690–700. Available at: <http://dx.doi.org/10.1016/j.proeng.2013.09.144>.
- Tsai, M.Y. et al., 2015. Investigation of milling cutting forces and cutting coefficient for aluminum 6060-T6. *Computers & Electrical Engineering*, 000, pp.1–11.

Available at: <http://linkinghub.elsevier.com/retrieve/pii/S0045790615003237>.

Wang, C. et al., 2014. Research on the Chip Formation Mechanism during the high-speed milling of hardened steel. *International Journal of Machine Tools and Manufacture*, 79, pp.31–48. Available at: <http://linkinghub.elsevier.com/retrieve/pii/S0890695514000091>.

Appendix C

600 SFM Cutting Speed From Dyno-Ware



Appendix D

700 SFM Cutting Speed From Dyno-Ware

